Oligonucleotide Analogues with Integrated Bases and Backbone

Part 22[1])

Synthesis and Association of Thiomethylene-Linked Self-Complementary AUAU and UAUA Tetramers

by **Bruno Bernet**, **Zeena Johar**, **Anne Ritter**, **Bernhard Jaun***, and **Andrea Vasella***

Laboratory of Organic Chemistry, Department of Chemistry and Applied Biosciences, ETH Zürich, Wolfgang Pauli-Strasse 10, CH-8093 Zürich (e-mail: vasella@org.chem.ethz.ch)

The tritylated and silylated self-complementary A*[s]U*[s]A*[s]U* and U*[s]A*[s]U*[s]A* tetramers **18** and **24**, linked by thiomethylene groups (abbreviated as [s]) between a nucleobase and C(5′) of the neighbouring nucleoside unit were prepared by a linear synthesis based on *S*-alkylation of 5′-thionucleosides by 6-(chloromethyl)uridines, **7** or **10**, or 8-(chloromethyl)adenosines, **12** or **15**. The tetramers **18** and **24** were detritylated to the monoalcohols **19** and **25**, and these were desilylated to the diols **20** and **26**, respectively. The association of the tetramers **18**–**21** and **24**–**26** in $CDCl_3$ or in $CDCl_3$/(D_6)DMSO 95:5 was investigated by the concentration dependence of the chemical shifts for H–N(3) or H_2N–C(6). The formation of cyclic duplexes connected by four base pairs is favoured by the presence of one and especially of two OH groups. The diol **20** with the AUAU sequence prefers reverse-*Hoogsteen*, and diol **26** with the UAUA sequence *Watson–Crick* base pairing. The structure of the cyclic duplex of **26** in $CDCl_3$ at 2° was derived by a combination of AMBER* modeling and simulated annealing with NMR-derived distance and torsion-angle restraints resulting in a *Watson–Crick* base-paired right-handed antiparallel helix showing large roll angles, especially between the centre base pairs, leading to a bent helix axis.

Introduction. – In the course of exploring oligoribonucleotide analogues wherein the backbone of oligonucleotides is replaced by linking elements between nucleobases (ONIBs [2]), we investigated the pairing of the self-complementary U*[s]A$^{(*)}$ and A*[s]U$^{(*)}$ dinucleosides[2]) **1**–**5** (*Fig. 1*) [3]. Their pairing, *i.e.,* their association to form cyclic duplexes, depends on the sequence, and on whether the CH_2OH groups of units I and II are protected or not. Thus, the U*[s]A$^{(*)}$ alcohols **1** and **2** possessing a C(5′/II)OH or a C(8)CH_2OH group form preferentially cyclic duplexes, while the fully protected analogues **3** form only linear duplexes and higher associates. In the A*[s]U$^{(*)}$ series, only the alcohol **4** forms (mainly) cyclic duplexes, whereas the dinucleosides **5** lead predominantly to linear duplexes and higher associates, irrespectively of whether

[1]) Part 21: [1].

[2]) *Conventions for abbreviated notation:* The substitution at C(6) of pyrimidines and C(8) of purines is denoted by an asterisk (*); for example, U* and A* for hydroxymethylated uridine and adenosine derivatives, respectively. U$^{(*)}$ and A$^{(*)}$ represent both unsubstituted and hydroxymethylated nucleobases. The moiety x linking C(6)–CH_2 or C(8)–CH_2 (of unit II) and C(5′) (of unit I) is indicated in square brackets, *i.e.*, [c] for a C-atom, [o] for an O-, and [s] for a S-atom.

HO–C(5′/II) is protected or not. The conformations of the cyclic duplexes of these dinucleosides have been analysed, while the influence of the terminal CH_2OH groups has not been explored in similarly detailed way [3].

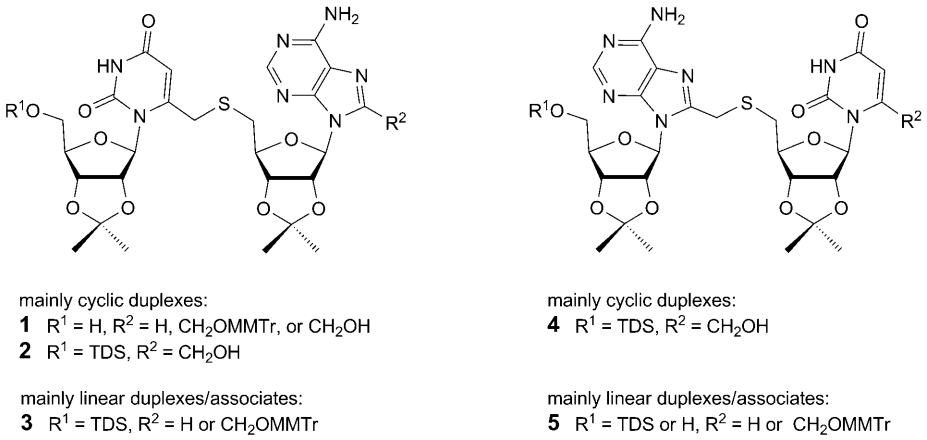

Fig. 1. *The self-complementary U*[s]A(*) dimers* **1** *and* **2** *and the A*[s]U(*) dimer* **4** *prefer the formation of cyclic duplexes, whereas the U*[s]A(*) dimers* **3** *and the A*[s]U(*) dimer* **5** *form mainly linear duplexes and higher associates.* TDS = (thexyl)(dimethyl)silyl (thexyl = 1,1,2-trimethylpropyl), MMTr = (monomethoxy)trityl = (4-methoxyphenyl)diphenylmethyl.

In continuing the exploration of thiomethylene-linked ONIBs it appeared of interest to analyse the pairing of the self-complementary U*[s]A*[s]U*[s]A* and A*[s]U*[s]A*[s]U* tetranucleosides to further assess the effect of the terminal OH groups on pairing, to test for an extrapolation of the previous conformational analysis, and to gain information about the cyclic duplexes. We describe the synthesis of these tetranucleosides, the analysis of their association, and the structure of one of the duplexes.

Results and Discussion. – 1. *Synthesis of the A*[s]U*[s]A*[s]U* and U*[s]A*[s]U*[s]A* Tetranucleosides.* The synthesis is based on the nucleophilic substitution, by a thiol or thiolate anion, of uridine or adenosine derivatives possessing a C(6) or C(8) halogenomethyl group, respectively. We opted for a linear rather than a convergent strategy, as it requires fewer building blocks. Four building blocks (*Scheme 1*) are required for the linear synthesis of a tetramer (or a higher oligomer). Two building blocks corresponding to the terminal unit I (*Schemes 2* and *3*) possess a C(5′)SH and a protected hydroxymethyl group at C(6) or C(8), and act exclusively as nucleophile. Two building blocks corresponding to the internal units II and III of the tetramer possess a protected thiol and a halogenomethyl group, and act in sequence as electrophile and as nucleophile. Two further monomers corresponding to unit IV possess a halogenomethyl and a protected hydroxy group at C(5′), and act solely as electrophile. Exploratory experiments showed that protection of the thiol group by acetylation is appropriate, as the thiol group can be regenerated by treatment with

K_2CO_3 in MeOH without affecting the AcS group at C(5′) of the electrophilic monomer under the conditions (K_2CO_3 in DMF) of the nucleophilic substitution.

Scheme 1

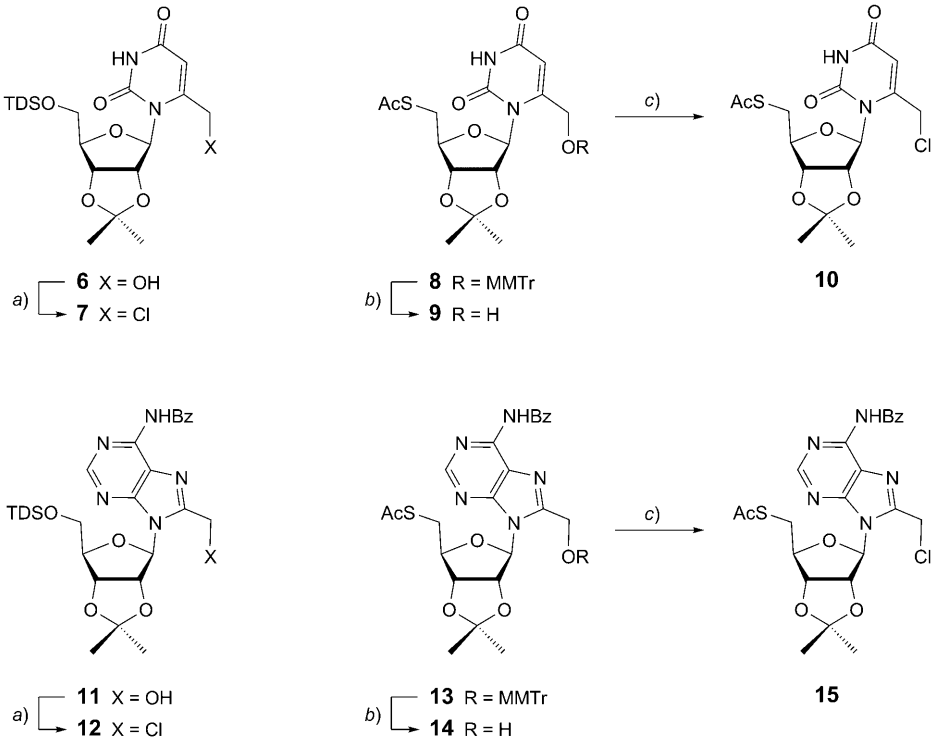

a) $MeSO_2Cl$ (MsCl), 4-(dimethylamino)pyridine (DMAP), CH_2Cl_2; 74% of **7**; 91% of **10**; 61% of **12**; 96% of **15**. *b*) Cl_2CHCO_2H, Et_3SiH, CH_2Cl_2; 73% of **9**; 96% of **14**. TDS = thexyldimethylsilyl (thexyl = 1,1,2-trimethylpropyl), MMTr = (monomethoxy)trityl = (4-methoxyphenyl)diphenylmethyl.

The preparation of the monomers **8**, **15**, **10**, and **12**, required for the synthesis of the A*[s]U*[s]A*[s]U* tetramer, and of the additional building blocks **13** and **7**, required for the U*[s]A*[s]U*[s]A* sequence isomer, is shown in *Scheme 1*. The monomers **7** and **12** corresponding to units IV were obtained in 74 and 61% yield, respectively, by treating the known alcohols **6** and **11** [3] with MsCl and 4-(dimethylamino)pyridine (DMAP) in CH_2Cl_2.

The tritylated thioacetates **8** and **13** corresponding to unit I are known [3]. Their detritylation with $Cl_2CHCOOH$ and Et_3SiH in CH_2Cl_2, followed by treatment of the resulting alcohols **9** and **14** with MsCl and DMAP in CH_2Cl_2, gave the chlorides **10** (66%) and **15** (92%), respectively, corresponding to units II and III of the tetramers.

The ^{1}H- and ^{13}C-NMR data of **7**, **9**, **10**, **12**, **14**, and **15** are listed in *Tables 4* and *5* in the *Exper. Part*. The chemical shift for H–C(2′) of the uridines **7**, **9**, and **10** in $CDCl_3$ at 5.25–5.26 ppm evidences the *syn*-orientation of the nucleobase. In the adenosine

series, only the silyl ether **12** (δ(H–C(2′)) = 5.83 ppm) adopts completely the *syn*-conformation, whereas substantial amounts of the *anti*-conformer of the thioacetates **14** (5.63 ppm) and **15** (5.74 ppm) are revealed by an upfield shift for H–C(2′), in agreement with earlier observations [3]. A 1:1 equilibrium of the *gt*- and *tg*-conformers of the uridine and adenosine derived thioacetates **9**, **10**, **14**, and **15** is deduced from *J*(4,5′a) and *J*(4,5′b) values of 6.9–7.5 Hz, whereas slightly smaller values for the silyl ether **12** (6.0 and 5.7 Hz) reveal a minor contribution of the *gg*-conformer. Signal overlap of the silyl ether **7** prevented the determination of the rotameric equilibrium.

The synthesis of the A*[s]U*[s]A*[s]U* tetramer **21** started by forming dimer **16** (*Scheme 2*). It was obtained in a yield of 67% by substituting the chloride **15** under basic conditions with the thiol obtained upon deacetylation of the trityl ether **8**. Similarly, trimer **17** was prepared in a yield of 42% by deacetylating **16** and treating the resulting thiol with the chloride **10**. Deacetylation of **17** and reaction with the chloride **12** resulted in 44% of the tetramer **18**. Debenzoylation of **18** with MeONa in MeOH gave the diamine **19** (65%) that was detritylated to the mono-alcohol **20** (24%). Desilylation of **20** with $(HF)_3 \cdot Et_3N$ in THF led to the desired diol **21** (38%). Yields were not optimised. The products **16**–**20** were purified by flash chromatography. This resulted in losing up to 30% of the products, on account to their low solubility in solvents allowing chromatographic separation. HPLC on several types of silica gel and gel permeation chromatography did not lead to improvements, and **21** was purified by repeated trituration with hexane, again entailing loss of material.

The sequence-isomeric U*[s]A*[s]U*[s]A* tetramer **26** was synthesized similarly to **21** (*Scheme 3*). Substitution of chloride **10** by the thiol derived from **13** gave the dinucleoside **22** (94%), substitution of chloride **15** by the thiol derived from **22** gave the trinucleoside **23** (> 98%), and substitution of chloride **7** by the thiol derived from **23** gave the benzoylated tetranucleoside that was directly debenzoylated to the diamine **24** (28%). Detritylation of **24** gave the mono-alcohol **25** (60%) that was desilylated to the diol **26** (35%). Finally, **26** was deisopropylidenated by the action of aqueous CF_3CO_2H in CH_2Cl_2 to yield 52% of the fully deprotected tetranucleoside **27**. Purification of the diamine **24** by chromatography on silica gel entailed loss of material. The mono-alcohol **25** was purified by trituration with MeOH, and the diol **26** and the polyol **27** by trituration with acetone.

^{1}H- and ^{13}C-NMR data of **16**–**27** are listed in *Tables 6*–*9* in the *Exper. Part*. In $CDCl_3$, the dimers **16** and **22** give rise to sharp signals, whereas the trimers **17** and **23** and especially the tetramers **18**–**21** and **24**–**26** give rise to strong line broadening due both to their poor solubility and to association. Therefore, we recorded spectra of solutions of the tetramers **20**, **21**, **24**, and **25** in (D_6)DMSO. In this solvent, the tetramers are completely solvated monoplexes, as evidenced by δ(H–N(3)) of 11.40–11.41 ppm and δ(H_2N–C(6)) of 6.68–7.32 ppm, values that are similar to those for H–N(3) of uridine mononucleosides (11.37–11.44 ppm [4][5]) and for H_2N–C(6) of adenosine mononucleosides (7.32–7.40 ppm [4][6]). The ^{1}H-NMR spectrum of **26** in $CDCl_3$ at 25° shows very broad lines, sharpened by lowering the temperature to 2°, but not sufficiently so as to detect couplings of less than 2 Hz. However, the resolution was sufficient to allow investigating the association by the analysis of DQF-COSY, TOCSY, and NOESY spectra (see below). The polyol **27** is insoluble in $CDCl_3$, and the NMR spectra were recorded in (D_6)DMSO. The NMR data compiled in *Tables 6*–*9* agree

Scheme 2

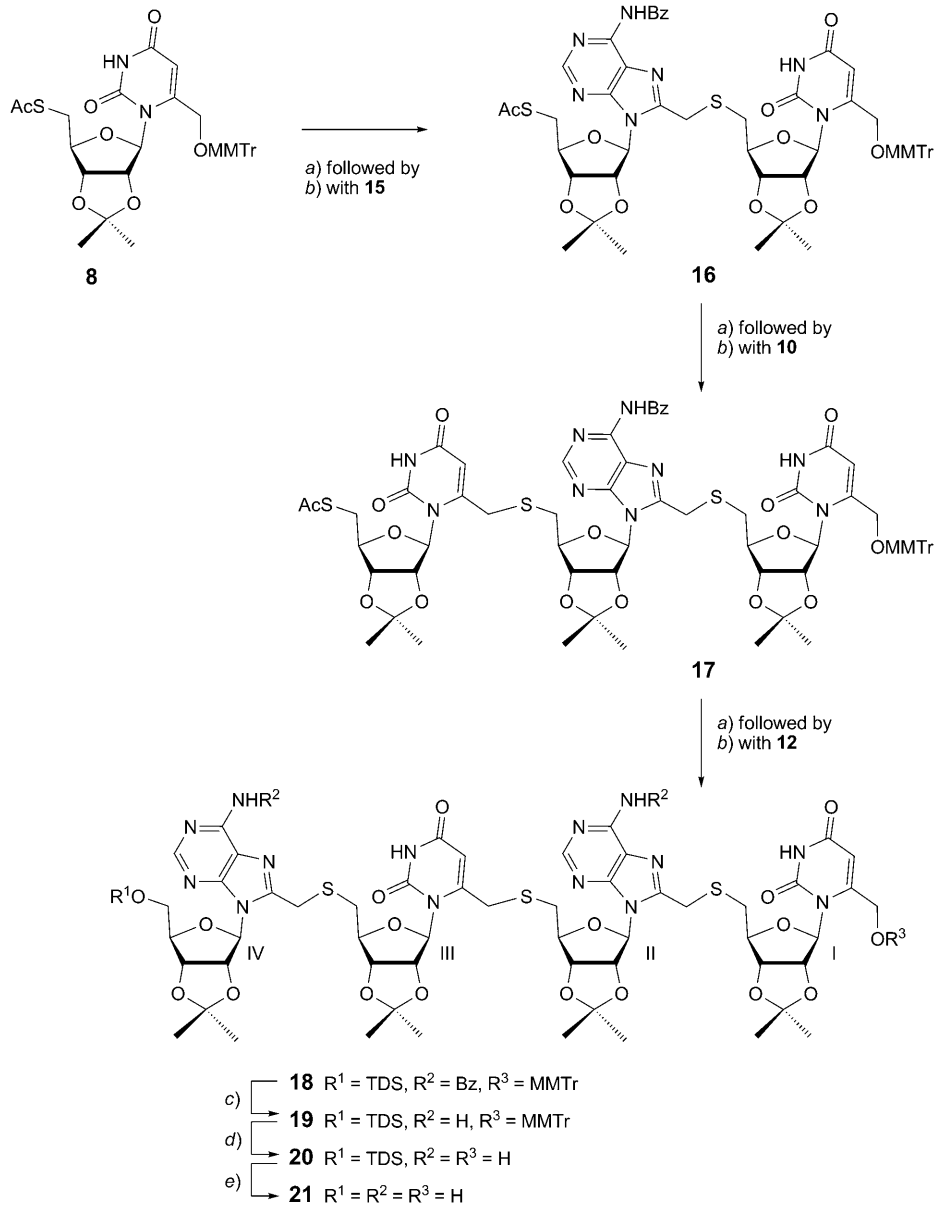

a) K_2CO_3, MeOH. *b*) Chloro compound, K_2CO_3, DMF; 67% of **16**; 42% of **17**; 44% of **18**. *c*) MeONa, MeOH; 65%. *d*) Cl_2CHCO_2H, Et_3SiH, CH_2Cl_2; 24%. *e*) $(HF)_3 \cdot Et_3N$, THF; 38%. TDS = (thexyl)(dimethyl)silyl, MMTr = (monomethoxy)trityl.

Scheme 3

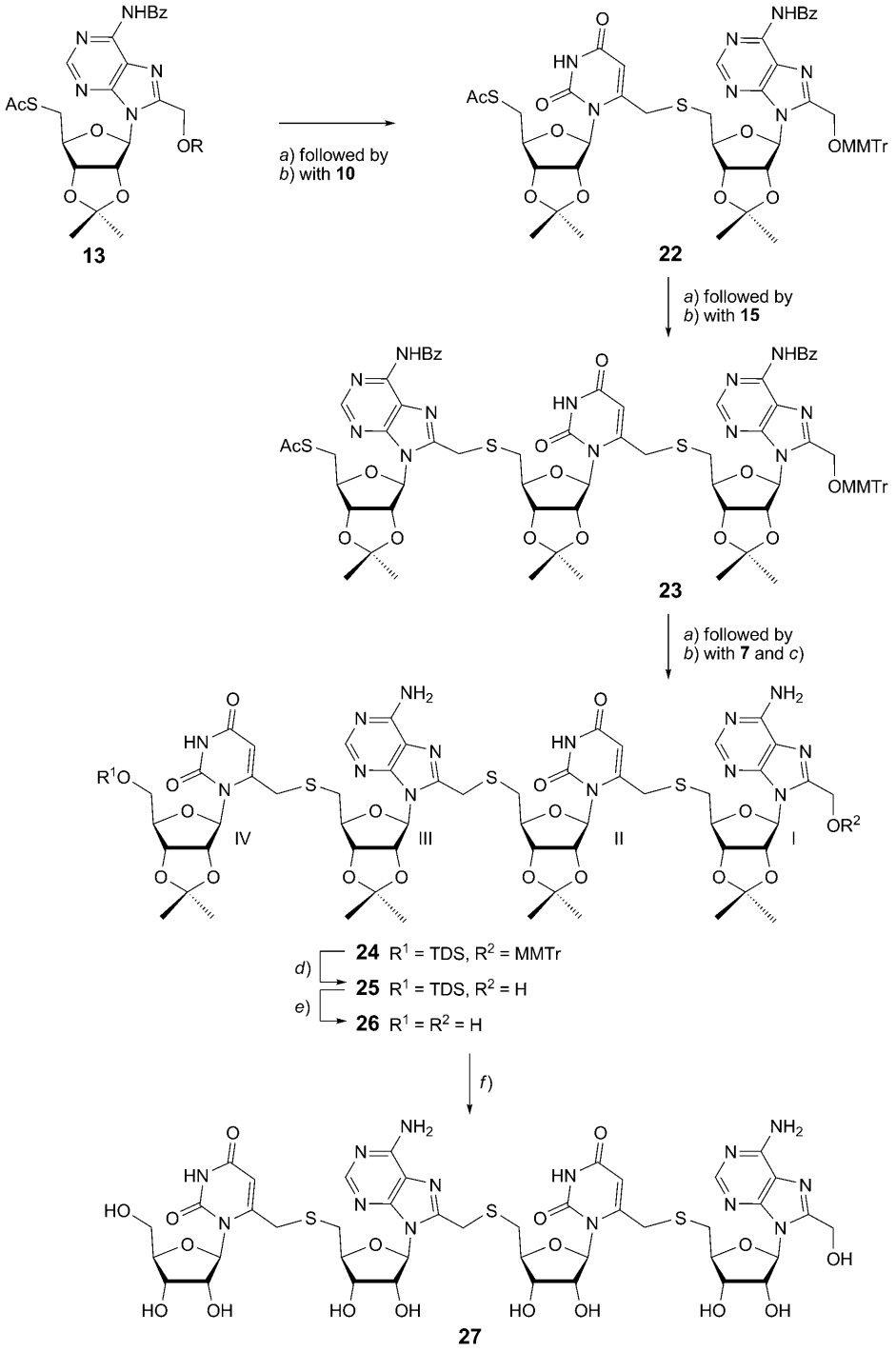

a) K_2CO_3, MeOH. *b*) Chloro compound, K_2CO_3, DMF; 94% of **22**; >98% of **23**. *c*) MeONa, MeOH; 28% of **24**. *d*) Cl_2CHCO_2H, Et_3SiH, CH_2Cl_2; 60%. *e*) $(HF)_3 \cdot Et_3N$, THF; 35%. *f*) CF_3CO_2H, H_2O, CH_2Cl_2; 52%. TDS = (thexyl)(dimethyl)silyl, MMTr = (monomethoxy)trityl.

well with the proposed structures. Data that are relevant for the analysis of the association are discussed in the next chapter.

2. *Association of the A*[s]U*[s]A*[s]U* and U*[s]A*[s]U*[s]A* Tetranucleosides.* The self-association of the A*[s]U*[s]A*[s]U* tetramers **19**–**21** and of the U*[s]A*[s]U*[s]A* tetramers **24**–**26** in $CDCl_3$ and in $CDCl_3/(D_6)DMSO$ mixtures was investigated by ^{1}H-NMR spectroscopy. The ^{1}H-NMR spectra of solutions of these tetramers in $CDCl_3$ at 25° show broad signals, evidencing association kinetics on the NMR time-scale. Despite the broad signals, we could determine the concentration dependence of the chemical shifts for H–N(3) of both uracil units of **19**, **21**, and **25**, resulting in 'shift concentration curves' (SCCs; *cf.* [3]). The tetramers are less well soluble than the corresponding dimers, and this restricted the analysis of the concentration dependence to lower concentrations (up to 15 mM) for the mono-alcohols and the diols. The SCCs of **19** and **20** in $CDCl_3/(D_6)DMSO$ 95 : 5 at ambient temperature, and of **24** and **25** in $CDCl_3$ at 50° were analysed numerically according the method of *Gutowsky* and *Saika* [7].

2.1. *Association of the A*[s]U*[s]A*[s]U* Tetranucleosides.* H–N(3/a) and H–N(3/b)[3]) of the dibenzamide **18** (15 mM solution in $CDCl_3$) that was not expected to form a cyclic duplex resonate at 10.20 and 9.73 ppm (*Table 1*), similarly as H–N(3) of the analogous U*[s]U* dimer (10.56 and 9.96 ppm [8]). These chemical shifts evidence an equilibrium between the monoplex and linear U · U duplexes, although a small contribution of linear and cyclic duplexes possessing *Hoogsteen*-type base pairing cannot be excluded. Debenzoylation of **18** to **19** led to a strong downfield shift of the H–N(3/a) and H–N(3/b) signals, now resonating at 13.03 and 12.38 ppm, and evidencing the formation of cyclic duplexes possessing *Watson–Crick*-type H-bonded base pairs. A comparison with δ(H–N(3/I)) of the corresponding tritylated A*[s]U* dimer (13.02 ppm [3]) may suggest that the H–N(3/a) signal of **19** at 13.03 ppm corresponds to H–N(3/I), and the one of H–N(3/b) at 12.38 to H–N(3/III). Detritylation of **19** to **20** leads to an upfield shift of both H–N(3) signals to 11.75 ppm, revealing a preference for reverse *Hoogsteen* base pairing, as it was found for the corresponding A*[s]U* dimer [3]. In agreement with this change of pairing mode, H–C(2) of **20** resonates upfield to H–C(2) of **19** (8.20/8.24 *vs.* 8.30/8.50 ppm). Reverse *Hoogsteen*-type base pairing appears to be favoured by an intramolecular H-bond of $HOCH_2$–C(6/I) to O–C(2′/I). The upfield shift for both H–N(3) of diol **21** (11.29 and 11.14 ppm) reveals the exclusive formation of reverse *Hoogsteen* base pairs.

Table 1. *Chemical Shifts* [ppm] *of H–N(3) of the A*[s]U*[s]A*[s]U* Tetramers* **18**–**21** *and the U*[s]A*[s]U*[s]A* Tetramers* **24**–**26** *for 10–15 mM Solutions in $CDCl_3$ and at 25°* (values in parenthesis at −20°)

	18	**19**	**20**	**21**	**24**	**25**	**26**
H–N(3/a)	10.20	13.03	11.75	11.29	(12.11)	12.70 (12.86)	14.11 (H–N(3/IV)
H–N(3/b)	9.73	12.38	11.75	11.14	(12.03)	11.86 (12.06)	13.03 (H–N(3/II)

[3]) The two H–N(3) signal of **18**–**21**, **24**, and **25** were not assigned to the individual uridine units. The more deshielded H–N(3) signal is labeled H–N(3/a) and the other one H–N(3/b).

The SCCs for the two H–N(3) signals of **19** in $CDCl_3$ are shown in *Fig. 2,a.* The SCC for H–N(3/a) and its downfield shift evidence the presence of cyclic duplexes already at a low concentration by the absence of a curvature below 10 mM and nearly constant chemical-shift values above 10 mM. The SCC for H–N(3/b) increases slightly from 12.33 to 12.40 ppm upon increasing the concentration from 7.5 to 32 mM; at concentrations below 7.5 mM, the H–N(3/b) signal is not visible. In contradistinction, the SCC for H–N(3/I) shows decreasing shift values, from 13.10 ppm at 2.2 mM to 12.94 ppm at 32 mM. This decrease suggests a further association of the cyclic duplexes with increasing concentration (*cf.* [8]).

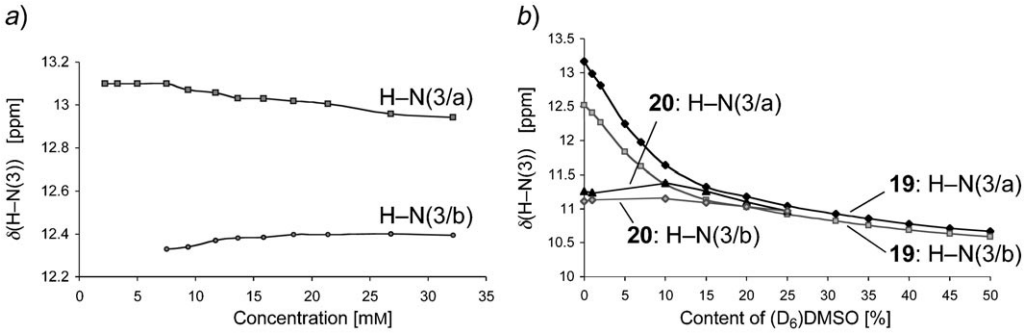

Fig. 2. a) *SCCs for H–N(3/a) and H–N(3/b) of* **19** *in $CDCl_3$ solution.* b) *Influence of the (D_6)DMSO content upon the chemical shift of H–N(3/a) and H–N(3/b) of* **19** *and* **20** *in $CDCl_3$ solution.*

The preference of diol **21** to form cyclic duplexes in $CDCl_3$ is evidenced by a slight increase of δ(H–N(3/a)) (from 11.22 to 11.29 ppm) and of δ(H–N(3/b)) (from 11.03 to 11.14 ppm) with increasing concentration (from 5.5 to 13.9 mM). Like the SCC of **19** (*Fig. 2,a*), the one of **21** in $CDCl_3$ (not shown) shows no curvature at low concentrations, preventing a quantitative analysis of the association.

Adding increasing amounts of (D_6)DMSO to $CDCl_3$ solutions of self-complementary dinucleosides shifts the monoplex $\rightleftharpoons$ duplex equilibrium progressively in favour of the (solvated) monoplex [9]. Upon addition of 50% of (D_6)DMSO, δ(H–N(3/a)) and δ(H–N(3/b)) of **19** decrease from 13.70 to 10.70, and from 12.53 to 10.59 ppm, respectively. The lines parallel to the two branches of the curves depicting the solvent dependence of the chemical shift of H–N(3a and b) (*Fig. 2,b*) cross at a $CDCl_3$/(D_6)DMSO ratio of *ca.* 9:1, suggesting complete solvation, *i.e.*, the presence exclusively of the monoplex at a (D_6)DMSO content of 10%. As H–N(3) of a reverse *Hoogsteen* base-paired cyclic duplex and H–N(3) of a completely solvated monoplex in (D_6)DMSO resonate at a similar field (*ca.* 11 ppm), one expects at best a weak solvent dependence upon adding increasing amounts of (D_6)DMSO to solutions of **20** and **21** in $CDCl_3$. This was indeed observed. The curves depicting the solvent dependence for δ(H–N(3)) for **20** (*Fig. 2,b*) show a weak increase upon adding 10% of (D_6)DMSO ($\Delta\delta$(H–N(3)) = 0.12 and 0.04 ppm). Coalescence prevented the determination of δ(H–N(3) at a 2–7% content of (D_6)DMSO. Above a content of 10% (D_6)DMSO, we observed a steady decrease of δ(H–N(3) up to a 50% content of (D_6)DMSO ($\Delta\delta$(H–N(3)) = 0.31 and 0.18 ppm). This corresponds to the expected

shift change for the transition of a *Hoogsteen*-type base-paired duplex to a solvated monoplex. Both H–N(3) of **21** in $CDCl_3$ resonate as a single very broad singlet at 11.22 ppm. Similarly as for **19**, a steady if weak decrease of this chemical shift was observed upon adding increasing amounts of (D_6)DMSO ($\Delta\delta = 0.14$ ppm after addition of 40% of (D_6)DMSO), also in agreement with the dissociation of a *Hoogsteen*-type base-paired duplex.

The above experiments show that the monomethoxytrityl ether **19** and the corresponding alcohol **20** form a monoplex $\rightleftharpoons$ duplex equilibrium in $CDCl_3$/(D_6)DMSO 95:5. This mixed solvent appeared well suited for the purpose of determining the association constants. The numerical analysis [7] of the SCCs depicted in *Fig. 3* led to a similar value of *ca.* 10.8 ppm for the chemical shift of H–N(3/b) = H–N(3/III) of **19** and **20**, extrapolated to a concentration of 0 mM (*Table 2*). For H–N(3/a) = H–N(3/I) of **19** and **20**, there is a difference of 0.3 ppm between the δ(H–N(3/I), $c = 0$ mM) values which may be at least partly due to the different substitution at C(6/I). A larger contribution of *Hoogsteen*-type H-bonded duplexes for **20** than for **19** is suggested by the upfield shift for H–N(3) of **20** ($\Delta\delta$(H–N(3), $c = \infty$) ≈ 0.4 ppm for both NH). The association constants K_{ass} calculated from δ(H–N(3/I) of **19** and **20** (310 and 251 M^{-1}, resp.) are larger than those calculated from δ(H–N(3/III) (126 and 115 M^{-1}, resp.), but the difference is within the large variance of the values. The SCCs for H–N(3/a) and H–N(3/b) of the diol **21** in $CDCl_3$/(D_6)DMSO 95:5 show a small and steady increase of the chemical shift upon increasing the concentration from 3.2 to 7.7 mM ($\Delta\delta \leq 0.06$ ppm), preventing numerical analysis. These differences evidence a large contribution of (reverse) *Hoogsteen* H-bonded cyclic duplexes in the association equilibrium of **21** (*cf.* [3]).

To further probe the association of these tetramers, we investigated the temperature dependence of the H–N(3) signals of the fully *O*-protected **19** (15.8 mM in $CDCl_3$; *Fig. 4*). At 40°, H–N(3/I) and H–N(3/III) resonate as broad *singlet*s at 12.5 and

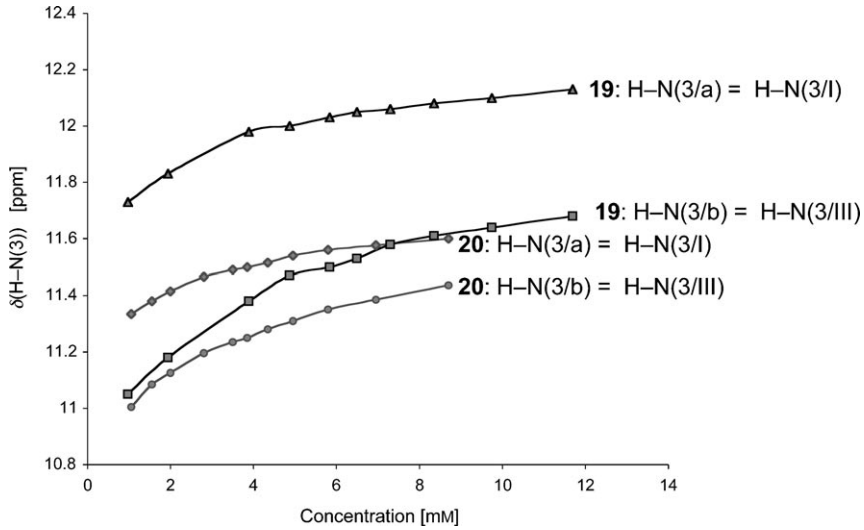

Fig. 3. *SCCs for both H–N(3) of* **19** *and* **20** *in $CDCl_3$/(D_6)DMSO 95:5*

Table 2. *Numerical Analysis of the SCCs of the A*[s]U*[s]A*[s]U* and U*[s]A*[s]U*[s]A* Tetramers* **19**, **20**, **24**, *and* **25** *in* Fig. 2, b, *and* Fig. 4: *Calculated* ^{1}*H-NMR Chemical Shifts* [ppm] *of H–N(3) or of* H_2N*–C(6) of the Monoplex* ($c = 0$ mM) *and of the Cyclic Duplexes* ($c = \infty$), *and Calculated Association Constants* K_{ass} [M^{-1}]

	19	**20**	**25**	**24**
Solvent Temperature	$CDCl_3/(D_6)DMSO$ 95 : 5 25°	$CDCl_3/(D_6)DMSO$ 95 : 5 25°	$CDCl_3$ 50°	$CDCl_3$ 50°
	H–N(3/a)	H–N(3/a)	H–N(3/a)[a])	H_2N–C(6/c)[b])
δ ($c = 0$ mM) δ ($c = \infty$) K_{ass}	11.42 ± 0.17 12.44 ± 0.09 310 ± 253	11.12 ± 0.07 11.90 ± 0.06 251 ± 118	7.69 ± 0.06 11.89 ± 0.04 6523 ± 1403	5.85 ± 0.06 7.04 ± 0.08 456 ± 172
	H–N(3/b)	H–N(3/b)	H–N(3/b)[a])	H_2N–C(6/d)
δ ($c = 0$ mM) δ ($c = \infty$) K_{ass}	10.76 ± 0.13 12.41 ± 0.22 126 ± 74	10.80 ± 0.05 12.07 ± 0.12 115 ± 43	7.70 ± 0.05 11.60 ± 0.04 3630 ± 479	5.85 ± 0.37 7.07 ± 0.14 259 ± 333

[a]) Including a value of 7.70 ppm for 0.0001 mM. [b]) Including a value of 5.85 ppm for 0.0001 mM.

11.85 ppm, respectively. They coalesce and disappear at 0°, and reappear at −20° as two broad *singlet*s at 14.05 and 13.7 ppm, respectively. At −40°, two rather sharp *singlet*s at 14.15 and 13.75 ppm evidence a single cyclic duplex possessing *Watson–Crick*-type base pairs. The H–N(3) signals of the monoplex are expected at a somewhat lower field than those of H–N(3) of the monoplex at room temperature (7.7 ppm [3]), considering the expected downfield shift due to cooling to −40°. Five broad *singlet*s integrating for 5 H appear between 7.9 and 8.5 ppm at temperatures below the coalescence temperature. They have to be assigned to the associated NH atoms of the H_2N–C(6/II and IV) groups of the cyclic duplex, and to H–N(3/I and III) and H–C(2/II and IV) of the monoplex, whereas H–C(2/II and IV) of the cyclic duplex resonate at −40° as sharp *singlet*s at 8.72 and 8.47 ppm.

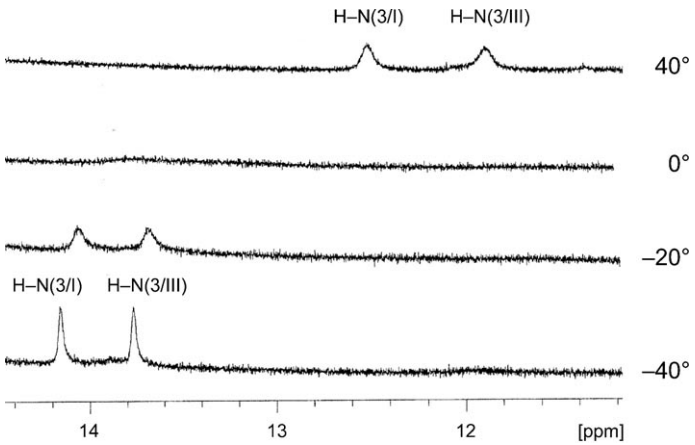

Fig. 4. *Temperature dependence of the H–N(3) signals of* **19** *for a 15.8 mM solution in* $CDCl_3$

For the mono-alcohol **20**, we expected *Watson–Crick*- and *Hoogsteen*-type base-paired duplexes. H–N(3/a) and H–N(3/b) of **20** resonate as two rather sharp *singlet*s at 10.82 and 10.47 ppm at 50°, and at 20° as one broad *singlet* at 11.7 ppm. At –10 to –40°, coalescence was observed. The chemical shift of H–N(3/a and b) at 20° agrees well with an equilibrium of *Watson–Crick*- and *Hoogsteen*-type base-paired cyclic duplexes.

Unfortunately, solutions of **21** in $CDCl_3$ gave rise to broad signals both at 25° and 2°; no NOESY cross-peaks between NH and other H signals could be detected. The structure of the reverse *Hoogsteen* H-bonded cyclic duplex of **21** was modeled (AMBER* in Macromodel v. 6.0 [10]) by extending the structure of the cyclic duplex of the corresponding A*[s]U* dimer [3], and fixing the distances of all H-bonds and the torsion angles of the linking CH_2SCH_2 moieties. This led to a rather regular right-handed A helix with *ca.* seven residues per turn (*Fig. 5*). After releasing all constraints, the AMBER*-modeled structure showed large propeller and buckle twists that result from avoiding a close contact between O=C(4) of U and $ROCH_2$–C(8) of A. This may be an artifact, as suggested by *ab initio* calculation (*Spartan 2004: Hartree-Fock* calculation with the 3-21G basis set [11]) of a reverse *Hoogsteen* base pair of uracil with 8,9-dimethyladenine that suggests a binding interaction between O=C(4) of uridine and H_3C–C(8) of 8,9-dimethyladenine[4]). There is (on the basis of modeling), therefore, no reason to doubt the reverse *Hoogsteen* base pairing of **21**.

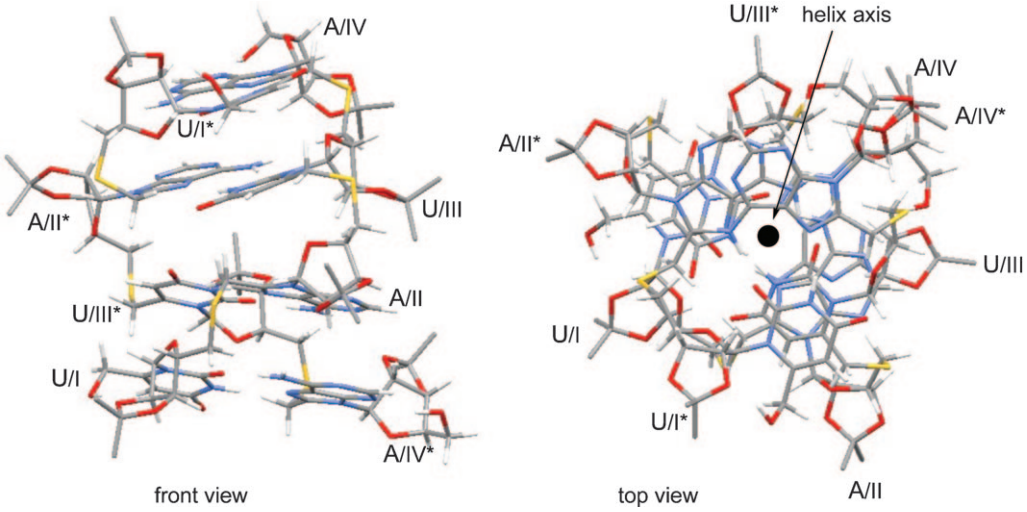

Fig. 5. *AMBER*-Modelled* (using constraints for the H-bond distances and the torsion angles of the CH_2SCH_2 linking units) *cyclic duplex of the diol* **21** *connected by reverse*-Hoogsteen *base pairing* (H-atoms of isopropylidene groups omitted for enhanced clarity; units of the complementary strand marked with a star)

---

4) C–H···O=C H-bonds in β-sheets of proteins were evidenced by ^{h3}J(C,C) scalar couplings [12]. Their calculated association enthalpy ΔH^{298} of –3 kcal/mol corresponds roughly to half the size of the association enthalpy of a N–H···O=C H-bond [13].

2.2. *Association of the U*[s]A*[s]U*[s]A* Tetranucleosides.* The H–N(3) signals of the fully *O*-protected analogue **24** (10–15 mM in $CDCl_3$) could not be observed at 25° due to coalescence. They appear at −20° at 12.11 and 12.03 ppm (*Table 1*). The two H–N(3) of the mono-alcohol **25** resonate at −20° at 12.86 and 12.06 ppm, and at 25° at 12.70 and 11.86 ppm. At 25°, the two H–N(3) of the diol **26** resonate at 14.11 and 13.03 ppm revealing *Watson–Crick*-type H-bonded cyclic duplexes. The upfield shifts for the H–N(3) signals of **24** and **25** ($\Delta\delta = 1.2-2.2$ ppm) may be rationalized by an increasing contribution of *Hoogsteen*-type associated duplexes, or, similarly as it was observed for the corresponding U*[s]A* dimers [3], by an increasing contribution of linear duplexes and of the monoplex. 2D-NMR Experiments (see below) show that the more deshielded H–N(3/a) of **26** corresponds to H–N(3/IV), but do not settle the assignment of the H–N(3) signals of **24** and **25**. The uncertainty stems from a comparison of the chemical shifts for H–N(3) of **24**–**26** with those for the corresponding U*[s]A* dimers (12.5 mM $CDCl_3$) where H–N(3/II) resonates at 11.1, 11.9, and 12.8 ppm, respectively, suggesting that the more shielded H–N(3/b) of **26** corresponds to H–N(3/IV).

The H–N(3) signals of the mono-alcohol **25** in $CDCl_3$ at 25° are very broad. At 50°, however, the signals are rather sharp and allow determination of the concentration dependence. The SCC for H–N(3/a) of **25** (*Fig. 6,a*) shows the characteristic shape denoting an equilibrium between monoplex and one or several cyclic duplexes, *i.e.*, a strong curvature below 10 mM and a plateau above 15 mM. A weaker curvature of the SCC for H–N(3/b) of **25** suggests the formation also of minor amounts of linear duplexes. Numerical analysis of the SCCs led to reliable results only upon including a value of 7.70 ppm/0.0001 mM (*cf.* [3][14]), resulting in K_{ass} values of 6523 ± 1403 and 3630 ± 479 M^{-1} (*Table 2*). Assuming the same relative chemical shifts for H–N(3/II) and H–N(3/IV) of **25** as for **26** one may rationalize these results by an equilibrium between cyclic duplexes with all four units base-paired, and cyclic duplexes where only units III and IV pair. In such a partially paired duplex, H–N(3/a = IV) is completely involved in a base pair, and H–N(3/b = II) only partially so.

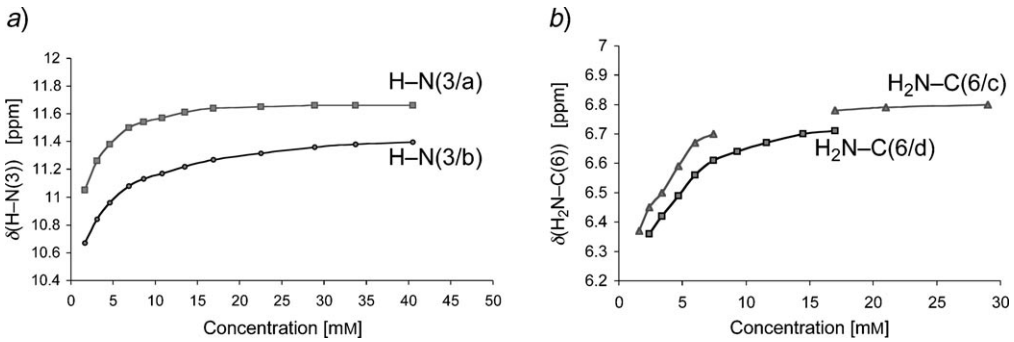

Fig. 6. a) *SCCs for H–N(3/a) and H–N(3/b) of* **25** *in $CDCl_3$ at 50°.* b) *SCCs for H_2N–C(6/a) and H_2N–C(6/b) of* **24** *in $CDCl_3$ at 50°.*

The temperature dependence of the ^{1}H-NMR spectra of **25** (12 mM in $CDCl_3$) between 22 and −40° (*Fig. 7*) evidences the predominant formation of a single

Watson–Crick base-paired cyclic duplex at −40°. At 22°, H–N(3/a = IV?) and H–N(3/b = II?) resonate as broad *singlet*s at 12.70 and 11.86 ppm, whereas the H_2N–C(6) signals are hidden due to coalescence. Lowering the temperature to 10° led to a weak downfield shift for H–N(3/a = IV?) and H–N(3/b = II?) ($\Delta\delta = 0.19$ and 0.26 ppm, resp.) and to the appearance of four NH_2 signals, *i.e.*, two signals at 9.54 and 9.46 ppm of associated H–N, and two signals at 7.55 and 6.55 ppm of free H–N. All these signals became sharper upon cooling to −10°[5]). While these six NH signals evidence a single, *Watson–Crick* base-paired cyclic duplex, additional very weak H–N(3) signals (at 11.8, 12.3, 12.55, and 13.2 ppm, −40°) suggest a small contribution of two other *Watson–Crick*-type base-paired cyclic duplexes.

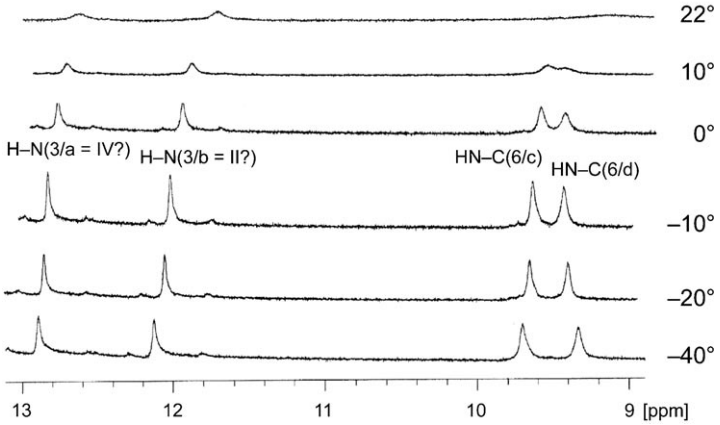

Fig. 7. *Temperature dependence of the H–N(3) and HN–C(6) signals of* **25** *between 9 and 13 ppm for a 12-mM solution in $CDCl_3$*

A cyclic duplex of **25** (molecular mass 1439.73 g/mole) is further evidenced by the apparent molecular mass of 2850 ± 100 for a 10 mM solution in CH_2Cl_2, as determined by vapour pressure osmometry.

The H–N(3) signals of the fully *O*-protected **24** in $CDCl_3$ show coalescence at 25°. The signal is very broad at 50° and does not allow us to determine the concentration dependence of the chemical shift. For this reason, we followed the concentration dependence of the two H_2N–C(6) signals of the A(I and III) moieties at 50° which were only hidden between 6.72 and 6.77 ppm by the signals of the $MeOC_6H_4$ group (*Fig. 6,b*). In agreement with observations for adenosine-derived dimers [3], the two H_2N–C(6/c and d) signals (integrating for two H) were assigned to one H_2N–C(6) group each of the two adenosine moieties; they represent an average of H-bonded and free HN. Numerical analysis of the SCC for H_2N–C(6/d) led to a reliable result, with $\delta(H_2N\text{–}C(6),\ c = 0\ \text{mM})$ of 5.85 ± 0.37 ppm and $K_{ass} = 259 \pm 333\ \text{M}^{-1}$ (*Table 2*). Numerical analysis of the SCC for H_2N–C(6/c) also gave a reliable result upon

[5]) There is a weak influence of the temperature on the chemical shift for the associated NH upon cooling from 10 to −40°, *i.e.*, a weak downfield shift for H–N(3/a), H–N(3/b), and HN–C(6/c) ($\Delta\delta \leq 0.20$ ppm) and a weak upfield shift for HN–C(6/d) ($\Delta\delta = 0.13$ ppm). The chemical shift of the free NHs is hardly influenced by the temperature ($\Delta\delta \leq 0.03$ ppm).

including a value of 5.85 ppm/0.0001 mM, with $K_{ass} = 456 \pm 172$ M^{-1}. These approximate values evidence a weak association of the fully *O*-protected **24**, similarly to the corresponding U*[s]A* dimer ($K_{ass} = 227$ M^{-1} [3]), although the values are based on signals representing an average of H-bonded and free H of the NH_2 groups (*cf.* [8]).

The H–N(3) signals of the diol **26** in $CDCl_3$ at 27° appear at 14.11 and 13.03 ppm, independently of the concentration (2–10 mM). This evidences a strong association ($K_{ass} \geq 10^4$ M^{-1}). The broad H–N(3) signals of **26** disappear in the noise upon progressive dilution of a 12 mM solution in $CDCl_3/(D_6)DMSO$ 95:5 preventing a numerical determination of K_{ass}. The strong association suggested analyzing the structure of the duplex, and this required a detailed analysis of the ^{1}H-NMR spectra.

2.2.1. *Qualitative Analysis of the ^{1}H-NMR Data of the Diol* **26** *in $CDCl_3$ at 2°*. At 2°, the resolution of the ^{1}H-NMR spectra of a 5 mM solution of **26** in $CDCl_3$ was sufficient to allow investigating the associated structure by analysis of DQF-COSY, TOCSY, and NOESY spectra. An unambiguous assignment of the signals was only feasible by a combined analysis of these spectra.

The signals of the U units II and IV were unambiguously assigned by TOCSY cross-peaks between H–N(3) and H–C(5), intra-units ROESY cross-peaks between H–C(5) and CH_2–C(6), CH_2–C(6) and H–C(1′), and H–C(1′) and H–C(4′), and TOCSY cross-peaks between H–C(1′) and H–C(2′), and between H–C(4′) and $H_2C(5')$. Similarly, the CH_2–C(8) signals of the A units I and III were correlated by NOESY and DQF-COSY cross-peaks with the corresponding $H_2C(5')$ signals. The H–C(2) signals were assigned on the basis of weak NOESY cross-peaks with the corresponding H–C(3′) signals.

Only the H_2N–C(6) signals could not be assigned by intra-unit cross-peaks. They resonate as two pairs of *singlet*s at 9.15/7.47 and 7.97/5.66 ppm, the non-equivalence of the H-atoms of both NH_2 groups evidencing the formation of a stable cyclic duplex connected by four base pairs. The pairs of *singlet*s were assigned by DQF-COSY and TOCSY cross-peaks. The individual signals were assigned with the help of inter-unit NOESY cross-peaks of H–N(3/IV) and H–N(3/II). H–N(3/IV) shows cross-peaks with the NH_2 signals at 9.15/7.47 ppm and the H–C(2/I) signal at 8.38 ppm, and H–N(3/II) shows cross-peaks with the other NH_2 group at 7.97/5.66 ppm and the H–C(2/III) signal at 7.94 ppm. In addition, both H–N(3) signals show exchange-NOESY cross-peaks with both OH signals at 5.77 and 4.68 ppm, and with HDO at 1.80 ppm. The cross-peaks with H–C(2) evidence *Watson–Crick* or reverse *Watson–Crick* base pairing between units I and IV, and between units II and III. As expected from the strong downfield shift of both H–N(3) signals, there is no evidence for *Hoogsteen*-type base pairing (no cross-peaks between H–N(3/IV) and CH_2–C(8/I) nor between H–N(3/II) and CH_2–C(8/III)).

HO–C(5′/IV) resonates as a *doublet* at 4.69 ppm. The downfield shift and the large coupling of 9.7 Hz is consistent with a rather persistent bifurcated H-bond to O=C(2/IV) and O–C(4′/IV) (*cf.* [3] and refs. cit. therein). *H*OCH_2–C(8/I) resonates as a *doublet* at 5.77 ppm. The large *J*(H,OH) value of 11.5 Hz evidences that the OH group is forming a H-bond, with H–O antiperiplanar to one C–H of the CH_2 group. This excludes an intramolecular H-bond to N(7/I), as this would require H–O to be in the σ-plane of the adenine moiety (torsion angle H–C–O–H $\pm 120°$), while an intramolecular H-bond to O–C(2′/I) agrees well with this coupling.

The combined analysis of the DQF-COSY, TOCSY, and NOESY spectra allowed us to unambiguously assign all ^{1}H-NMR signals of **26** in $CDCl_3$ at 2° (see *Table 8* in the *Exper. Part*). There are several unexpected chemical shifts that must be due to anisotropy effects in the cyclic duplex. One notes a strong upfield shift of H–C(5/II) (4.77 ppm; $\Delta\delta \approx 1$ ppm), an upfield shift for H–C(2/III) (7.94 ppm; $\Delta\delta \approx 0.4$ ppm), a strong upfield shift for H–C(1′/IV) (5.23 ppm; $\Delta\delta > 0.6$ ppm), a downfield shift for H–C(2′/II) (5.49 ppm; $\Delta\delta \approx 0.3$ ppm), upfield shifts for H–C(2′/I) (5.05 ppm; $\Delta\delta >$ 0.45 ppm) and H–C(2′/III) (5.20 ppm; $\Delta\delta > 0.3$ ppm), a downfield shift for H–C(3′/I) (5.41 ppm; $\Delta\delta \approx 0.3$ ppm), a downfield shift for H–C(4′/I) (4.65 ppm; $\Delta\delta \approx$ 0.3 ppm), and an upfield shift for H–C(4′/IV) (3.90 ppm; $\Delta\delta \approx 0.4$ ppm)[6]). Large shift differences (0.47–0.86 ppm) are found for the geminal H-atoms of CH_2–C(8/III), CH_2–C(6/II), CH_2–C(6/IV), H_2C(5′/I), H_2C(5′/III), and H_2C(5′/IV), evidencing a strongly anisotropic environment. The geminal H-atoms of CH_2–C(8/I) and H_2C(5′/II), however, show only a weak $\Delta\delta$ of 0.11–0.13 ppm.

The *syn*-orientation of all nucleobases in the duplex of **26** is evidenced by NOESY cross-peaks between H–C(1′) and CH_2–C(6 or 8), and corroborated by NOESY cross-peaks between H–C(3′) and H–C(2) of the adenosine units. Hence, the upfield shift observed for H–C(2′/I) and H–C(2′/III) must indeed be due to anisotropy effects and does not denote an *anti*-orientation of the adenosine unit. A northern (*N*) conformation is evidenced for units I–III by DQF-COSY cross-peaks between H–C(3′) and H–C(4′), and by the absence of DQF-COSY cross-peaks between H–C(1′) and H–C(2′); line broadening prevents the exact determination of the $J(1',2')/J(3',4')$ ratio. Unit IV, however, shows a preference for a southern (*S*) conformation, evidenced by DQF-COSY cross-peaks between H–C(1′/IV) and H–C(2′/IV). It is likely that this conformation is induced by the intramolecular bifurcated H-bond of HO–C(5′/IV) to O=C(2/IV) and O–C(4′/IV). NOESY Cross-peaks between the signals of *H*OCH_2–C(8/I) and both H–C(1′/I) and H–C(2′/I) confirm the intramolecular H-bond to O–C(2′/I).

A *gt*- or *tg*-orientation of the sulfanyl substituent of units I–III is evidenced by a large coupling of 10.2–10.8 Hz between H–C(4′) and the more strongly deshielded H_a–C(5′). The also expected small coupling of H–C(4′) with the less strongly deshielded H_b–C(5′) was not resolved. The *gt*- or *tg*-orientation of the sulfanyl group is corroborated by strong DQF-COSY cross-peaks between the H–C(4′) and H_a–C(5′) signals, and the absence of cross-peaks between H–C(4′) and H_b–C(5′). As expected for an *ap* orientation of H_a–C(5′) and H–C(4′), and a *gauche* orientation of H_b–C(5′) and H–C(4′), the NOESY spectrum shows weaker cross-peaks between the signals of H_a–C(5′) and H–C(4′) than between those of H_b–C(5′) and H–C(4′) (volume ratio *ca.* 1:1.5–2.0). However, both the H_a–C(5′) and H_b–C(5′) signals show cross-peaks with the H–C(3′) signal of similar intensity (volume ratio *ca.* 1:1). This is only compatible with a *gt*-conformation. Thus, the more strongly deshielded H_a–C(5′/

[6]) Some of these unexpected shifts may be rationalized on the basis of the calculated duplexes **26A**–**26C** (see below). The upfield shifts of H–C(5/II) and H–C(2/III) agree with their localisation in the shielding cone above A(I) and U(IV), respectively, whereas a downfield shift of H–C(2′/II) is expected from its position in the deshielding cone near the plane through U(II).

I–III) corresponds to H_{Re}, in agreement with the analogous assignment for H_a–C(5′/I) of the corresponding U*[s]A* dimer [3]. The intramolecular H-bond of HO–C(5′/IV) requires a *gg*-orientation. This conformation could not be corroborated by DQF-COSY and NOESY cross-peaks due to overlapping H–C(4′/IV) and H_a–C(5′/IV) signals.

In the absence of any coupling constants, the deduction of the approximate torsion angle about the H_2C–C(6 or 8) bond of the sulfanyl moiety has to rely on the relative NOE intensities of the two CH_2. In U(IV), both HC–C(6/IV) show a strong intraresidual NOE to H–C(1′/IV). This indicates that, in U(IV), both HC–C(6) point towards H–C(1′), and that the torsion angle N(1)–C(6)–CH_2–S is 180 ± 60°. With this general orientation it was possible to individually assign the two H_2C–C(6/IV); the one showing a NOE with H–C(2′/IV) was assigned to H_{Si}. For A(III) and U(II), a specific assignment was only possible *via* a cyclic process using the structures calculated with pseudo-atoms for H_2C–C(8 or 6) to deduce the assignment that is congruent with the observed NOEs.

2.2.2. *AMBER* Modeling of the Cyclic Duplex of* **26**. A rough calculation of the solution structure of **26** at 2° in $CDCl_3$ by simulated annealing with NMR-derived distance and torsion-angle restraints (programme *XPLORE-NIH*, version 2-0-4 [15]) led to 64 *Watson–Crick* base-paired structures showing neither NOE-distance (> 0.1 Å) nor torsion-angle violations (> 5°) [16]. The 14 structures lowest in energy had in common the *syn*-orientation of all nucleobases and the *tg*-orientation of all sulfanyl groups, but suffered from inefficient base pairing (evidenced by O···HN and NH···N distances of 1.51–1.84 and 2.02–2.81 Å, resp.), unfavourable propeller and buckle twists (up to 50°), free OH groups, and especially from poor base stacking (distance of 4.6–7.2 Å between the centre base pairs and of 3.5–5.6 Å between the border base-pairs). The conformation of the $H_2C(5')$–S–CH_2 linker between units I and II was similar to that between units II and III, but different from that between units III and IV. The structure showing the weakest propeller and buckle twists was selected for optimization with the programme AMBER* implemented in Macromodel v. 6 [10]. First, constraints were set for *Watson–Crick* base pairing, for the formation of the intramolecular H-bonds of the OH groups, and for a distance of 3.4 Å between the base pairs. In one calculation, the conformation of the $H_2C(5')$–S–CH_2 linkers was maintained, and in another calculation the conformation of the linker between units III and IV was brought in line with that of the other linkers. After this calculation, all constraints were released for the final optimisation. This led to the duplex stuctures **26A** and **26B** (5 kcal/mol lower in energy than **26A**), differing essentially in the conformation of the linker between units III and IV (*Fig. 8*). The front views of **26A** and **26B** show more or less parallel border base pairs and strongly inclined centre base pairs evidenced by roll angles[7]) of 4.9, 5.1, and 15.0° for **26A**, and of twice 5.7 and 15.2° for **26B**. Thus, only the border base pairs show base stacking (distance 3.20–3.25 Å). The strong inclination of the centre base pairs leading to a bent helix axis is presumably the result of backbone strain in these cyclic duplexes. The top views of **26A** and **26B**

[7]) Determined by measuring the angle between the two main planes through $C(2_U)$, $C(4_U)$, $C(6_U)$, $C(3_A)$, $C(6_A)$, and $C(8_A)$ of the two base pairs.

reveal a mean twist angle of *ca.* 60°, *i.e.*, six units per turn in a right-handed A helix possessing a central hole the size of a phenyl ring.

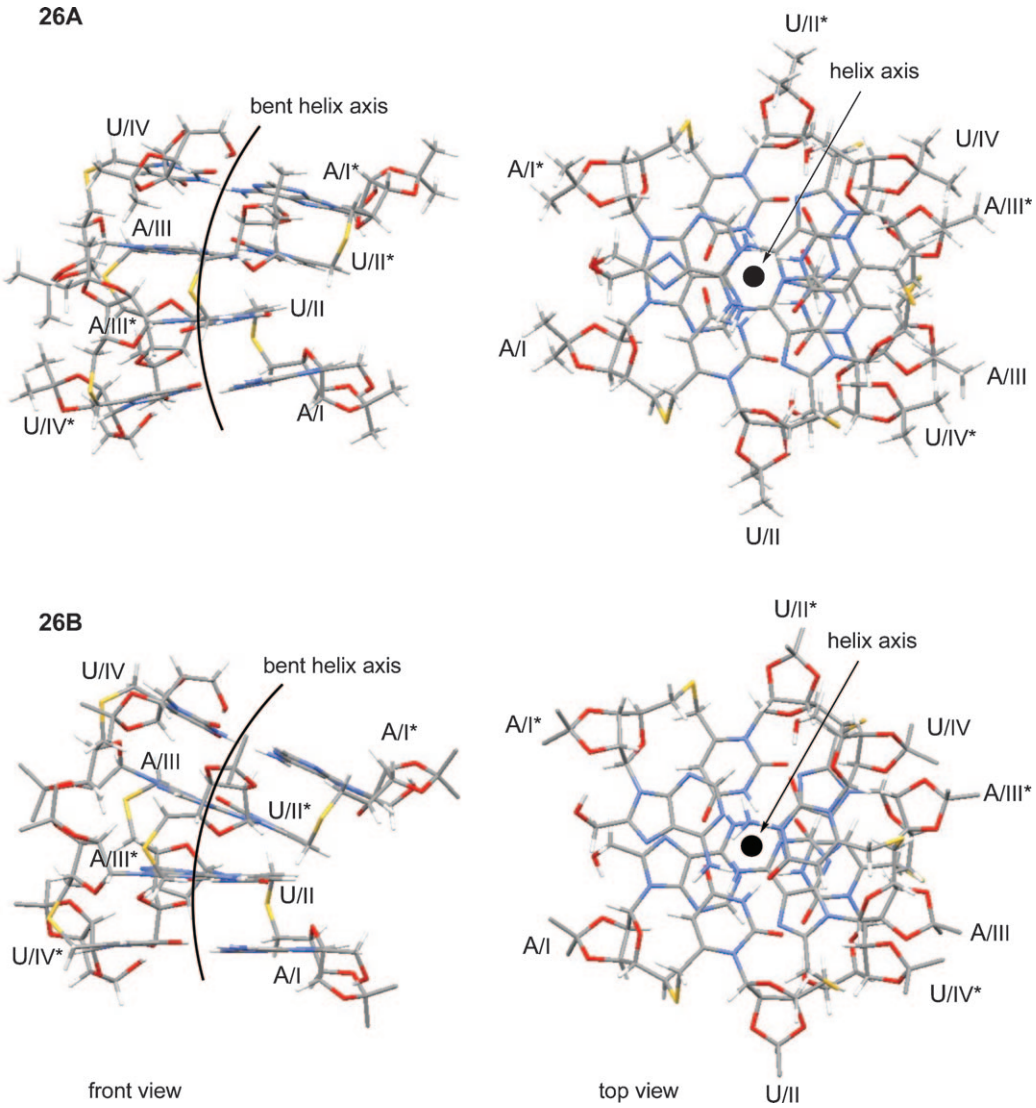

Fig. 8. *AMBER*-Modelled cyclic duplexes* **26A** *and* **26B** *connected by* Watson–Crick *base pairing* (H-atoms of isopropylidene groups omitted for enhanced clarity; units of the complementary strand marked with a star)

The structures of the duplexes **26A** and **26B** were analyzed in more detail (*Fig. 8* and *Table 3*). The strands are connected by four *Watson–Crick* base pairs (characterized by NH···N and NH···O distances of 1.75–1.76 Å) that show no or only weak

Table 3. *H-Bond Distances* [Å] *and Selected Torsion Angles* [°] *of the Cyclic Duplexes* **26A**, **26B**, *and* **26C** (obtained by AMBER* and XPLOR-NIH calculations, resp.).

H···X Bond		H···X Distance [Å]		
		26A	**26B**	**26C**
N(3)–H···N(1)		1.75, 1.78[a])	1.75	1.92, 2.05[a])
C(4)=O···HN–C(6)		1.78, 1.71[a])	1.76–1.77	2.16, 1.98[a])
OH···O(2′/I)		2.00	1.98	
OH···O=C(2/IV)		1.71	1.70	
OH···O(5′/IV)		2.33	2.43	
Torsion Angle	Short notation	Torsion angle [°][b])		
O(4′)–C(1′)–N(9)–C(4), unit I	χ/I	52.3	51.9	59.5
O(4′)–C(1′)–N(1)–C(2), unit II	χ/II	50.0	53.3	77.1
O(4′)–C(1′)–N(9)–C(4), unit III	χ/III	52.7	45.1	67.5
O(4′)–C(1′)–N(1)–C(2), unit IV	χ/IV	48.1	54.7	36.0
O(4′)–C(4′)–C(5′)–S, unit I	η_1/I	90.2	90.7	90.4
O(4′)–C(4′)–C(5′)–S, unit II	η_1/II	80.2	78.7	90.1
O(4′)–C(4′)–C(5′)–S, unit III	η_1/III	64.5	77.3	76.0
O(4′)–C(4′)–C(5′)–O, unit IV	η_1/IV	– 59.2	– 64.0	[c])
C(3′)–C(4′)–C(5′)–S, unit I	η_2/I	– 152.3	– 151.7	– 150.1
C(3′)–C(4′)–C(5′)–S, unit II	η_2/II	– 160.2	– 161.6	– 150.0
C(3′)–C(4′)–C(5′)–S, unit III	η_2/III	– 177.4	– 163.1	– 164.7
C(3′)–C(4′)–C(5′)–O, unit IV	η_2/IV	59.5	54.8	[c])
C(4′)–C(5′)–S–CH_2, unit I	θ/I	– 59.7	– 61.1	– 78.7
C(4′)–C(5′)–S–CH_2, unit II	θ/II	– 66.0	– 68.9	– 92.5
C(4′)–C(5′)–S–CH_2, unit III	θ/III	– 147.2	– 70.8	– 177.1
C(5′)–S–CH_2–C(6), unit I	ι/I	– 59.8	– 61.7	– 52.5
C(5′)–S–CH_2–C(8), unit II	ι/II	– 59.2	– 60.5	– 62.0
C(5′)–S–CH_2–C(6), unit III	ι/III	64.2	– 47.7	62.7
S–CH_2–C(6)–N(1), unit I	κ/I	– 61.2	– 61.8	– 73.4
S–CH_2–C(8)–N(9), unit II	κ/II	– 59.0	– 59.0	– 61.8
S–CH_2–C(6)–N(1), unit III	κ/III	– 162.6	– 60.7	– 149.9

[a]) First value: terminal units, second value: central units. [b]) Mean value of both strands ($\Delta\measuredangle \leq 0.4°$). [c]) Not determined (programme allows free rotation of the CH_2OH group).

propeller and buckle twists. All nucleobases adopt a *syn*-conformation (χ/I–IV 45–55°). The sulfanyl moieties of units I–III adopt a distorted *gt*-conformation. The distortion decreases from unit I (η_1/I *ca.* 90°) to units II (η_1/II *ca.* 80°) and to units III (η_1/III = 77° for **26B** and 64.5° for **26A**; see *Table 3* for the definition of the angles). The C(4′)–C(5′)–S–CH_2–C(6 or 8)–N(1 or 9) fragment of all linkers adopt a $g^-g^-g^-$ (torsion angles θ, ι, and κ) conformation, except for the linker between units II and III of **26A** which adopts a tg^+t-conformation. In agreement with the experimental data, the furanose rings of units II and III of **26A** and **26B** adopt a northern ^3E-conformation, while unit I adopts a southern ^2E-conformation, with a calculated $J(1,2) > 7.0$ Hz that is not in agreement with the experimental data. In the AMBER* calculation, the southern conformation is a consequence of the intramolecular H-bond to O–C(2′),

while *Maruzen* modeling suggests that this intramolecular H-bond is also compatible with a northern conformation[8]).

HO–C(5′/IV) of **26A** and **26B** forms an intramolecular H-bond to O=C(2/IV) rather than a bifurcated H-bond to O–C(4′/IV), as indicated by H···O distances of 1.71 and 1.70 *vs.* 2.33 and 2.43 Å, respectively (*Table 3*), whereas bifurcated (if strongly asymmetric) H-bonds are found in crystal structures of closely related uridine monomers (H···O distances of 1.71–1.83 and 2.15–2.37 Å [17–19]). This H-bond leads to a *gg*-orientation of the CH_2OH side chain and an E_1 furanose conformation, as also found in the X-ray structures.

Finally, the inter-proton distances of the minimized structures **26A** and **26B** were compared with the NOE-derived distance constraints. For both structures **26A** and **26B**, minimized with AMBER*, NOE back-calculations showed a number of large discrepancies (-1.2 Å $< d < +1.0$ Å) between the experimental NOE constraints and the corresponding distances in **26A** (13 violations ≥ 0.5 Å) and **26B** (24 violations ≥ 0.5 Å). Most of these violations involved the sequential distances across the sulfanyl linkers, and the relative intra-residual distances between the CH_2–C(6/8) and H–C(1′).

2.2.3. *Calculation of the Solution Structure of* **26** *in* $CDCl_3$ *at* 2° *by Simulated Annealing with NMR-Derived Distance and Torsion-Angle Restraints.* A total of 288 cross-peaks from the NOESY, $t_m = 300$ ms, spectrum of **26** in $CDCl_3$ at 2° were integrated, and the volumes converted into distance restraints using the two-spin approximation (for details, see *Exper. Part*). The torsion angles C(3′)–C(4′)–C(5′)–S were restricted to $180 \pm 20°$ based on vicinal couplings between H–C(4′) and H_{Re}–(C5′). Because the downfield shift of H–N(3) clearly indicated the presence of four base pairs, *Watson–Crick* base pairing was enforced by additional distance restraints across the H-bonds. Starting with a loose and extended antiparallel duplex, a total of 97 structures were calculated according to the torsion-angle-simulated annealing molecular-dynamics protocol of *Stein et al.* with the programme XPLOR-NIH [15]. A small subset of five NOEs that involved the terminal OH H-atoms (NOEs between units A(I) and U(IV)) was consistently violated in all initial structure calculations. Because of possible contributions of chemical exchange between the OH H-atoms, these NOEs were omitted from the final calculations. It is conceivable that these weak NOEs originate from end-to-end association of duplexes mediated through H-bonds involving the terminal OH groups, but, in view of the sparse data available, this question has to remain open.

Since qualitative analysis of the NMR data did not allow us to definitely decide between *Watson–Crick* (*WC*) and reverse *Watson–Crick* (r*WC*) base pairing, all four C_2-symmetric patterns of base pairing with *WC* or r*WC* base pairs (*WC*-*WC*-*WC*-*WC*, *WC*-r*WC*-r*WC*-*WC*, r*WC*-*WC*-*WC*-r*WC*, r*WC*-r*WC*-r*WC*-r*WC*) were calculated separately. However, all three variations with r*WC* base pairs generated only structures with severe violations of experimentally derived distance or dihedral angle restraints,

---

8) AM1, but not AMBER* modeling suggested also a conformation in which the C–O bond of the OH is in the π-plane of the adenine moiety, and O–H is parallel to the C(8)=N(7) bond. This conformer agrees with J(H,OH) = 11.5 Hz, but not with the NOESY cross-peaks between the signal of *H*OCH_2–C(8/I), and of both H–C(1′/I) and H–C(2′/I) signals.

whereas, for the duplex with four *WC* base pairs, 65 out of the 97 calculated structures did not show any violations of the distance or torsion-angle contraints. A bundle of all accepted structures, aligned based on the S-atoms, is shown in *Fig. 9,a*, and the structure **26C** with the lowest calculated energy in the bundle is depicted in *Fig. 9,b–d*, from different view angles.

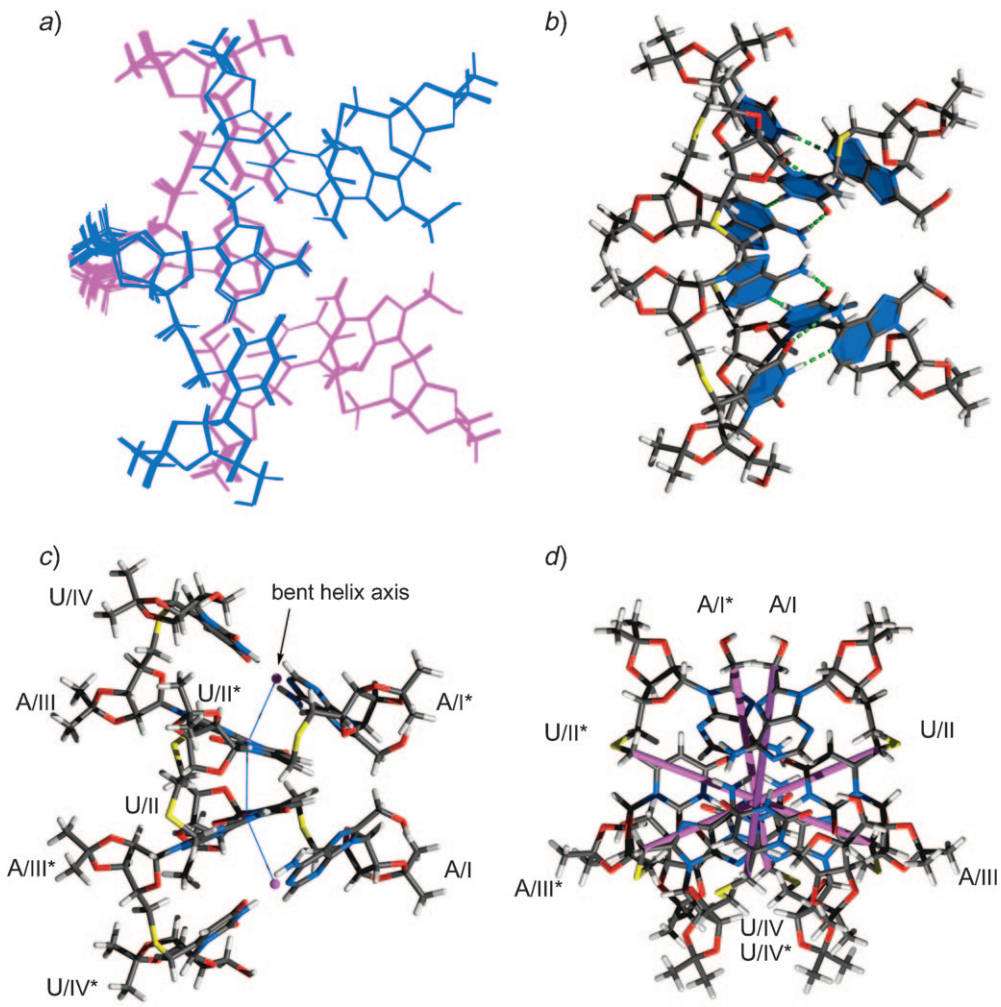

Fig. 9. *Structure of the Watson–Crick base-paired cyclic duplex* **26C** *as calculated with the NMR-derived contraints for* **26** *in CDCl$_3$ at 2°. a*) Bundle of all 67 accepted structures (rmsd = 0.057 Å). *b*) Single (lowest calculated energy) structure from the bundle in a view perpendicular to the C_2 axis. *c*) View showing the strong roll leading to a pronounced helix curvature. The purple spheres are the centres of each base pair (midpoint of the line connecting the two exocyclic CH_2–C(6/8)) of opposite bases. *d*) Top view of the helix showing the twists between the base pairs. The purple cylinders connect the two exocyclic CH_2–C(6/8) of opposite bases.

With such a short duplex of only four base pairs, a standard geometrical analysis of the helix parameters is impossible, because the helix axis is not well-defined. Hence, the following description has to remain qualitative. In $CDCl_3$, **26C** forms an antiparallel duplex with four *Watson–Crick* base pairs in a right-handed, strongly bent helix fragment (*Fig. 9,b*). The estimated twist angles are 60° between the terminal and 45° between the centre base pairs (*Fig. 9,d*)[9]).

The most striking feature of **26C** is the very pronounced roll of the base pairs, in particular between the two centre ones (roll angle of 39.5°)[7]), whereas the roll angle between the border base pairs is *ca.* 22° (*Fig. 9,d*). This large and unidirectional roll leads to a strong curvature of the helix axis. A polygon drawn through the centers of the base pairs (midpoints between the two CH_2–C(8/6)) does not approximate a straight line (as, *e.g.*, in B-type DNA) but exhibits a curvature with a radius of *ca.* 10 Å (see *Fig. 9,c*). Although all neighbouring base pairs approach each other to *Van der Waals* distance at one point, the large roll between the central base pairs prevents efficient base stacking and opens a cleft in the overall shape of the duplex that is best seen from the CPK model shown in *Fig. 10*. The strong curvature of the helix axis of **26C** predicts that duplex formation of the homologous self-complementary hexamers and octamers is not feasible due to disturbing steric interactions of the terminal A units.

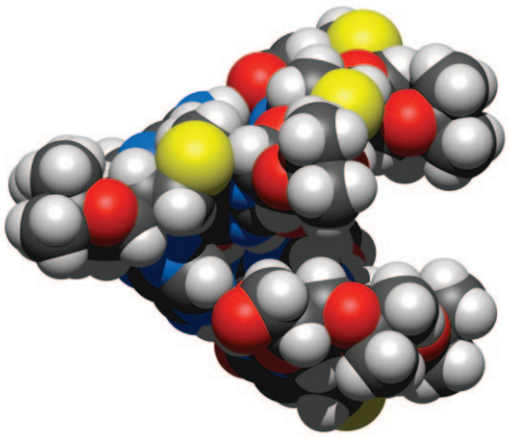

Fig. 10. *CPK Representation of the* Watson–Crick *base-paired cyclic duplex* **26C** *showing the pronounced cleft in the overall shape*

The structure of **26C** was analyzed in more details (*Table 3*). It forms *Watson–Crick* base pairs with N(3)H···N(1) and C(4)=O···HN–C(6) distances of 1.92 and 2.15 Å for the border base pairs, and 2.05 and 1.98 Å, respectively, for the centre base pairs. The structure adopted by **26C** is similar to the one of the AMBER* modeled **26A**, possessing a *syn*-orientation of the nucleobases, a *gt*-orientation of the sulfanyl substituents, a $g^-g^-g^-$ (torsion angles θ, ι, and κ) conformation of the C(4′)–C(5′)–S–CH_2–C(6 or 8)–N(1 or 9) fragment of the linkers between units I

[9]) In its geometrical definition, the twist as seen in this figure is not identical to the twist of a standard helix (linear helix axis) as defined for DNA and RNA.

and II, and units II and III, and a tg^+t-conformation of this linking fragment between units III and IV. Thus, relatively small differences of the angles χ, and $\eta-\kappa$ are mainly responsible for the different puckering of **26A** and **26C**. In agreement with the experimental $J(1',2')$ and $J(3',4')$ values, the furanose rings of units I–III adopt a northern ($^3H_2$ or $3E$) and those of unit IV an ^OE conformation.

The diastereotopic HOCH_2(5′/IV) and HOCH_2–C(8/I) cannot be assigned by the SPARKY programme [20], due to overlapping H–C(4′/IV) and H_a–C(5′/IV) signals, and to poor NOESY interactions of HOCH_2–C(8/I). Hence, XPLOR-NIH calculation cannot predict the conformation of the CH_2OH groups established by the large J(H,OH) values (see above), but leads to freely rotating CH_2OH groups.

The broadening of all ^{1}H-NMR signals of **26** in $CDCl_3$ at 2° excludes the presence of a single conformer, but may indicate an equilibrium of the easily interconvertible duplexes **26A** and **26C** (but with intramolecular H-bonds of the OH groups) and/or aggregation of the cyclic duplexes. Indeed, $J(5',OH) = 9.7$ Hz suggests a *ca.* 90% persistent intramolecular H-bond and would allow the aggregation of cyclic duplexes by an intermolecular H-bond of $HOCH_2C(5'/IV)$ to OCH_2–C(8/I). This could rationalize the five weak ROESY cross-peaks between the units A(I) and U(IV) that consistently violated all initial duplex structures of the XPLOR-NIH calculation.

2.2.4. *No Association of the Polyol* **27** *in* (D_6)*DMSO.* The completely deprotected polyol **27** proved insoluble in $CDCl_3$ and $CDCl_3$/(D_6)DMSO 9:1. In pure (D_6)DMSO, H–N(3) and H_2N–C(6) resonate at 11.34/11.31 and 7.29 ppm, respectively. These values are characteristic for U and A monomers in (D_6)DMSO [4–6] and evidence a completely solvated monoplex of **27** in (D_6)DMSO.

Conclusions. – The analysis of the sequence-isomeric self-complementary tetramers confirms the results obtained from the investigation of the corresponding dimers. In the U*[s]A*[s]U*[s]A* and U*[s]A* series, the diol forms exclusively a *Watson–Crick* base-paired cyclic duplex, with the tetramer showing the structure of an incipient A-helix, but possessing a bent helix axis, and, in the A*[s]U*[s]A*[s]U* and A*[s]U* series, the diols form a reverse *Hoogsteen* base-paired cyclic duplex. The OH groups at the terminal units strongly enhance the formation of cyclic duplexes.

We thank the *Swiss National Science Foundation, F. Hoffmann-La Roche AG*, Basel, and *Syngenta AG*, Basel, for generous support. *B. J.* and *Z. J.* thank the ETH Zürich for financial support (TH Project TH-17/02).

Experimental Part

General. See [3].

*6-(Chloromethyl)-5′-*O*-[dimethyl(1,1,2-trimethylpropyl)silyl]-2′,3′-*O*-isopropylideneuridine* (**7**). Under N_2, a soln. of **6** [3] (700 mg, 1.53 mmol) in CH_2Cl_2 (5 ml) at 0° was treated with DMAP (460 mg, 3.83 mmol) and MsCl (238 µl, 3.06 mmol), stirred for 1 h at 0 and for 2 h at 23°, diluted with CH_2Cl_2 (50 ml), and washed with sat. NH_4Cl soln., sat. $NaHCO_3$ soln., and brine. The combined org. phases were dried ($MgSO_4$) and evaporated. FC (AcOEt/cyclohexane 2:3) gave **7** (540 mg, 74%). R_f (AcOEt/cyclohexane 1:1) 0.50. $[\alpha]^{25}_D = -5.9$ ($c = 1.0$, $CHCl_3$). IR ($CHCl_3$): 3387*w*, 3189*w* (br.), 2961*m*, 2869*w*, 1700*s*, 1626*w*, 1461*m*, 1447*m*, 1379*m*, 1268*w*, 1256*w*, 1157*w*, 1131*w*, 1084*m*, 980*w*, 876*m*, 835*m*. ^{1}H-NMR (300 MHz, $CDCl_3$): see *Table 4*; additionally, 1.60 (*sept.*, $J = 6.9$, Me_2CH); 1.55, 1.31 (2*s*, Me_2CO_2); 0.86 (*d*, $J = 6.9$, Me_2CH); 0.83 (*s*, Me_2CSi); −0.07, −0.06 (2*s*, Me_2Si). ^{13}C-NMR (75 MHz, $CDCl_3$): see *Table 5*; additionally, 113.55 (*s*, Me_2CO_2); 34.08 (*d*, Me_2CH); 27.24, 25.34 (2*q*, Me_2CO_2); 25.26 (*s*,

Table 4. *Selected* ^{1}*H-NMR Chemical Shifts* [ppm] *and Coupling Constants* [Hz] *of the U* and A* Monomers* **7**, **9**, **10**, **12**, **14**, *and* **15** *in* $CDCl_3$

	7	**9**	**10**	**12**	**14**	**15**
H–C(2)	–	–	–	8.81	8.63	8.74
H–N(3) or HN–C(6)	9.16	9.35	10.45	8.94	9.53	9.16
H–C(5)	5.82	5.73	5.76	–	–	–
CH_a–C(6 or 8)	4.44	4.55	4.41	4.92	4.98–4.85	4.85
CH_b–C(6 or 8)	4.33	4.55	4.32	4.86	4.98–4.85	4.85
H–C(1′)	5.82	5.81	5.83	6.32	6.24	6.24
H–C(2′)	5.26	5.25	5.25	5.83	5.63	5.74
H–C(3′)	4.86–4.77	4.86	4.86	5.13	4.98	5.06
H–C(4′)	4.20–4.10	4.14	4.12	4.30	4.19	4.27
H_a–C(5′)	3.84–3.71	3.23	3.21	3.75	3.10	3.16
H_b–C(5′)	3.84–3.71	3.23	3.21	3.62	2.97	3.04
$J(CH_a,CH_b)$	13.2	[a])	12.9	15.3	[a])	[a])
J(1′,2′)	< 1.5	1.5	< 1.5	2.4	2.1	1.5
J(2′,3′)	6.0	6.3	6.3	6.3	6.3	6.3
J(3′,4′)	[a])	3.9	3.6	3.6	3.6	3.3
J(4′,5′a)	[a])	7.2	7.2	6.0	7.5	7.2
J(4′,5′b)	[a])	7.2	7.2	5.7	6.9	6.9
J(5′a,5′b)	[a])	[a])	[a])	11.9	13.8	13.8

[a]) Not assigned.

Table 5. *Selected* ^{13}*C-NMR Chemical Shifts* [ppm] *of the U* and A* Monomers* **7**, **9**, **10**, **12**, **14**, *and* **15**

	7	**9**	**10**	**12**	**14**	**15**
Solvent	$CDCl_3$	(D_6)DMSO	$CDCl_3$	$CDCl_3$	$CDCl_3$	$CDCl_3$
C(2)	150.57[a])	151.57	150.95[a])	152.58	152.46	153.24
C(4)	162.94	163.48	163.31	149.77	149.19	150.05
C(5)	104.62	101.67	105.11	122.26	121.70	122.49
C(6)	150.42[a])	155.59	150.76[a])	152.52	152.26	152.39
C(8)	–	–	–	150.06	154.81	150.05
CH_2–C(6 or 8)	41.09	60.03	41.29	36.73	57.55	36.64
C(1′)	91.67	91.33	92.26	90.42	89.92	90.43
C(2′)	84.20	85.16	85.23	83.24	84.04	84.09
C(3′)	81.91	84.43	84.48	81.59	83.86	83.95
C(4′)	89.62	87.97	88.69	87.65	86.61	86.97
C(5′)	63.83	31.69	31.58	62.83	31.26	31.30

[a]) Assignment may be interchanged.

Me_2CSi); 20.38, 20.22 (2*q*, *Me*$_2$CH); 18.54, 18.49 (2*q*, *Me*$_2$CSi); 3.23 (*q*, Me_2Si). HR-ESI-MS: 499.1823 (34), 498.1888 (24), 497.1839 (100, $[M+Na]^+$, $C_{21}H_{35}ClN_2NaO_6Si^+$; calc. 497.1851).

*5′-*S*-Acetyl-6-(hydroxymethyl)-2′,3′-*O*-isopropylidene-5-thiouridine* (**9**). A soln. of **8** [3] (150 mg, 0.23 mmol) in CH_2Cl_2 (3 ml) under N_2 was treated with Cl_2CHCO_2H (0.3 ml, 3.63 mmol) and Et_3SiH (75 µl, 0.47 mmol), and stirred for 15 min at 23°. The mixture was poured into sat. $NaHCO_3$ soln. After extraction with CH_2Cl_2, the combined org. phases were washed with brine, dried ($MgSO_4$), and evaporated. The residue was triturated with cyclohexane. Filtration gave **9** (63 mg, 73%). Colourless powder. R_f (AcOEt) 0.55. M.p. 202.6–203.7°. $[\alpha]^{25}_{D} = +10.7$ ($c = 1.0$, $CHCl_3$). IR (ATR): 3355*w*, 3195*w*,

3001*w*, 2987*w*, 2934*w*, 1686*s*, 1664*s*, 1617*w*, 1463*w*, 1421*w*, 1395*m*, 1385*m*, 1308*w*, 1275*w*, 1254*w*, 1238*w*, 1211*w*, 1157*w*, 1138*w*, 1101*s*, 1064*w*, 1042*s*, 1029*m*, 1003*m*, 983*w*, 972*w*, 952*w*, 865*m*, 855*s*, 831*m*, 805*m*. ^{1}H-NMR (300 MHz, $CDCl_3$): see *Table 4*; additionally, 3.12 (*t*, *J* = 6.0, OH); 2.34 (*s*, AcS); 1.52, 1.33 (2*s*, Me_2C). ^{13}C-NMR (75 MHz, (D_6)DMSO): see *Table 5*; additionally, 195.36 (*s*, SC=O); 113.34 (*s*, Me_2C); 31.17 (*q*, *Me*C=O); 27.61, 25.61 (2*q*, Me_2C). HR-MALDI-MS: 396.0923 (16), 395.0886 (100, $[M+Na]^+$, $C_{15}H_{20}N_2NaO_7S^+$; calc. 395.0883), 315.0641 (17), 273.1280 (15, $MMTr^+$, $C_{20}H_{17}O^+$; calc. 273.1279). Anal. calc. for $C_{15}H_{20}N_2O_7S$ (372.40): C 48.38, H 5.41, N 7.52; found: C 48.42, H 5.56, N 7.41.

5′-S-Acetyl-6-(chloromethyl)-2′,3′-O-isopropylidene-5′-thiouridine (**10**). Under N_2, a soln. of **9** (44 mg, 0.12 mmol) in CH_2Cl_2 (1 ml) at 0° was treated with DMAP (36 mg, 0.29 mmol) and MsCl (20 µl, 0.24 mmol), stirred for 10 min at 0 and for 2 h at 23°, and evaporated. A soln. of the residue in AcOEt was washed with sat. NH_4Cl soln. The combined org. phases were washed with brine, dried ($MgSO_4$), and evaporated. FC (AcOEt/cyclohexane 1:1) gave **10** (42 mg, 91%). Colourless foam. R_f (AcOEt/cyclohexane 4:1) 0.57. $[\alpha]^{25}_D = +0.5$ (*c* = 1.0, $CHCl_3$). IR ($CHCl_3$): 3386*w*, 3189*w* (br.), 3027*w*, 3014*w*, 2939*w*, 1698*s* (br.), 1627*w*, 1460*w*, 1447*w*, 1383*m*, 1272*w*, 1229*w* (br.), 1157*w*, 1136*w*, 1092*m*, 1063*m*, 982*w*, 909*w*, 875*w*, 836*w*. ^{1}H-NMR (300 MHz, $CDCl_3$): see *Table 4*; additionally, 2.30 (*s*, AcS); 1.49, 1.30 (2*s*, Me_2C). ^{13}C-NMR (75 MHz, $CDCl_3$): see *Table 5*; additionally, 195.05 (*s*, SC=O); 114.09 (*s*, Me_2CO_2); 30.80 (*q*, *Me*C=O); 27.26, 25.34 (2*q*, Me_2C). HR-MALDI-MS: 415.0511 (12), 413.0539 (38, $[M+Na]^+$, $C_{15}H_{19}ClN_2NaO_6S^+$; calc. 413.0545), 379.0932 (31, $[M-Cl+H+Na]^+$, $C_{15}H_{20}N_2NaO_6S^+$; calc. 379.0940), 333.0303 (17), 274.0426 (15), 273.1280 (100, $MMTr^+$, $C_{20}H_{17}O^+$; calc. 273.1279).

N^6-Benzoyl-8-(chloromethyl)-5′-O-[dimethyl(1,1,2-trimethylpropyl)silyl]-2′,3′-O-isopropylideneadenosine (**12**). Under N_2, a soln. of **11** [3] (1.000 g, 1.76 mmol) in CH_2Cl_2 (5 ml) was cooled to −10°, treated with DMAP (640 mg, 4.57 mmol) and MsCl (330 µl, 4.2 mmol), stirred for 10 min at 0 and for 3 h at 23°, diluted with CH_2Cl_2 (50 ml), and washed with sat. NH_4Cl soln., sat. $NaHCO_3$ soln., and brine. The combined org. phases were dried ($MgSO_4$) and evaporated. FC (AcOEt/cyclohexane 1:10 → 1:1) gave **12** (0.69 g, 61%). R_f (AcOEt/cyclohexane 1:1) 0.47. $[\alpha]^{25}_D = -18.3$ (*c* = 1.0, $CHCl_3$). IR ($CHCl_3$): 3408*w*, 3014*m*, 1709*m*, 1613*s*, 1589*m*, 1463*m*, 1360*m*, 1268*m*, 1089*s*. ^{1}H-NMR (300 MHz, $CDCl_3$): see *Table 4*; additionally, 8.00 (*d*, *J* = 7.8, 2 arom. H); 7.62–7.49 (*m*, 3 arom. H); 1.64, 1.42 (2*s*, Me_2CO_2); 1.57 (*sept.*, *J* = 6.9, Me_2CH); 0.84 (*d*, *J* = 6.9, Me_2CH); 0.79, 0.78 (2*s*, Me_2CSi); −0.004, −0.014 (2*s*, Me_2Si). ^{13}C-NMR (75 MHz, $CDCl_3$): see *Table 5*; additionally, 164.94 (*s*, C=O); 133.57 (*s*); 133.15 (*d*); 129.06 (2*d*); 128.22 (2*d*); 114.66 (*s*, Me_2CO_2); 34.25 (*d*, Me_2CH); 27.43, 25.63 (2*q*, Me_2CO_2); 25.47 (*s*, Me_2CSi); 20.46 (*q*, Me_2CH); 18.65 (*q*, Me_2CSi); −3.29 (*q*, Me_2Si). HR-MALDI-MS: 624.2381 (50, $[M+Na]^+$, $C_{29}H_{40}ClN_5NaO_5Si^+$; calc. 624.2385), 590.2764 (100, $[M-Cl+H+Na]^+$, $C_{29}H_{41}N_5NaO_5Si^+$; calc. 590.2775).

5′-S-Acetyl-N^6-benzoyl-8-(hydroxymethyl)-2′,3′-O-isopropylidene-5′-thioadenosine (**14**). Under N_2, a soln. of **13** [3] (100 mg, 0.13 mmol) in CH_2Cl_2 (2 ml) was treated with Cl_2CHCO_2H (0.2 ml, 2.4 mmol) and Et_3SiH (50 µl, 0.31 mmol) and stirred for 15 min at 23°. The mixture was poured into sat. $NaHCO_3$ soln. and extracted with CH_2Cl_2. The combined org. phases were washed with brine, dried ($MgSO_4$), and evaporated. FC (CH_2Cl_2/MeOH 100:0 → 95:5) gave **14** (62 mg, 96%). Foam. R_f (AcOEt) 0.28. $[\alpha]^{25}_D = -13.2$ (*c* = 1.0, $CHCl_3$). IR ($CHCl_3$): 3405*w*, 3030*w*, 2999*m*, 2940*w*, 1703*s* (br.), 1614*s*, 1590*m*, 1527*w*, 1480*s*, 1460*m*, 1427*m*, 1376*m*, 1356*m*, 1266*m* (br.), 1158*m*, 1134*m*, 1093*s*. ^{1}H-NMR (300 MHz, $CDCl_3$): see *Table 4*; additionally, 7.95 (*d*, *J* = 7.5, 2 arom. H); 7.48 (br. *t*, *J* = 7.5, 1 arom. H); 7.38 (*d*, *J* = 7.8, 2 arom. H); 6.05 (br. *s*, OH); 2.26 (*s*, AcS); 1.26, 1.37 (2*s*, Me_2C). ^{13}C-NMR (75 MHz, $CDCl_3$): see *Table 5*; additionally, 194.64 (*s*, SC=O); 165.42 (*s*, NC=O); 133.57 (*s*); 132.89 (*d*); 128.79 (2*d*); 128.10 (2*d*); 114.67 (*s*, Me_2C); 30.73 (*q*, *Me*C=O); 27.24, 25.51 (2*q*, Me_2C). HR-MALDI-MS: 523.1439 (27), 522.1412 (100, $[M+Na]^+$, $C_{23}H_{25}N_5NaO_6S^+$; calc. 522.1418), 500.1589 (16, $[M+H]^+$, $C_{23}H_{26}N_5O_6S^+$; calc. 500.1604).

5′-S-Acetyl-N^6-benzoyl-8-(chloromethyl)-2′,3′-O-isopropylidene-5′-thioadenosine (**15**). Under N_2, a soln. of **14** (62 mg, 0.12 mmol) in CH_2Cl_2 (1 ml) was cooled to 0°, treated with DMAP (37 mg, 0.31 mmol) and MsCl (20 µl, 0.24 mmol), and stirred for 1 h at 0 and for 3 h at 23°. The mixture was poured into sat. NH_4Cl soln. and extracted with CH_2Cl_2. The combined org. phases were washed with brine, dried ($MgSO_4$), and evaporated. FC (CH_2Cl_2/MeOH 100:0 → 95:5) gave **15** (62 mg, 96%). Colourless foam. R_f (AcOEt/cyclohexane 4:1) 0.46. $[\alpha]^{25}_D = +1.1$ (*c* = 1.0, $CHCl_3$). IR ($CHCl_3$): 3406*w*, 3014*m*, 2936*w*, 1707*s* (br.), 1613*s*, 1589*m*, 1525*w*, 1478*m*, 1463*m*, 1436*m*, 1424*m*, 1358*m*, 1329*m*, 1268*m*, 1249*m*, 1157*w*, 1134*m*, 1093*s*, 909*w*, 865*w*. ^{1}H-NMR (300 MHz, $CDCl_3$): see *Table 4*; additionally, 7.95 (*d*,

$J = 7.8$, 2 arom. H); 7.54 (br. *t*, $J = 7.5$, 1 arom. H); 7.45 (*d*, $J = 7.8$, 2 arom. H); 2.27 (*s*, AcS); 1.56, 1.36 (2*s*, Me_2C). ^{13}C-NMR (75 MHz, $CDCl_3$): see *Table 5*; additionally, 194.58 (*s*, SC=O); 164.91 (*s*, NC=O); 133.67 (*s*); 133.07 (*d*); 129.05 (2*d*); 128.13 (2*d*); 114.70 (*s*, Me_2C); 30.74 (*q*, *Me*C=O); 27.31, 25.54 (2*q*, Me_2C). HR-MALDI-MS: 540.1073 (23, $[M + Na]^+$, $C_{23}H_{24}ClN_5NaO_5S^+$; calc. 540.1079), 506.1481 (100, $[M - Cl + H + Na]^+$, $C_{23}H_{25}N_5NaO_5S^+$; calc. 506.1469).

5′-S-Acetyl-N^6-benzoyl-2′,3′-O-isopropylidene-5′-thioadenosine-8-methyl-(8^1 → 5′-S)-2′,3′-O-isopropylidene-6-{[(4-methoxyphenyl)diphenylmethoxy]methyl}-5′-thiouridine (**16**). Under N_2, a soln. of **8** (600 mg, 0.93 mmol) in O_2-free MeOH (2 ml) was treated with K_2CO_3 (400 mg, 2.79 mmol) and stirred for 10 min at 23°. Sat. NH_4Cl soln. (20 ml) was added, and the mixture was extracted with CH_2Cl_2. The combined org. phases were washed with brine, dried ($MgSO_4$), and evaporated. Under N_2, a soln. of the residue (500 mg, 0.83 mmol) in O_2-free DMF (2 ml) was treated with **15** (430 mg, 0.83 mmol) and K_2CO_3 (340 mg, 2.5 mmol), and stirred for 2 h at 23°. The mixture was poured into sat. NH_4Cl soln. and extracted with CH_2Cl_2. The combined org. phases were washed with brine, dried ($MgSO_4$), and evaporated. FC (AcOEt/cyclohexane 3:2 → 1:0) yielded **16** (606 mg, 67%). R_f (AcOEt/cyclohexane 7:3) 0.25. $[\alpha]^{25}_D = -19.7$ ($c = 1.0$, $CHCl_3$). IR ($CHCl_3$): 3395*w* (br.), 3200*w* (br.), 3015*m*, 2937*w*, 1697*s* (br.), 1612*m*, 1589*w*, 1510*w*, 1457*w*, 1423*w*, 1384*m*, 1356*w*, 1326*w*, 1299*w*, 1259*m* (br.), 1092*m*, 1062*m*. ^{1}H-NMR (300 MHz, $CDCl_3$): see *Table 6*; additionally, 10.81 (br. *s*, H–N(3/I)); 9.56 (*s*, HN–C(6/II)); 7.92 (*d*, $J = 8.4$, 2 arom. H); 7.49–7.24 (*m*, 15 arom. H); 6.79 (*d*, $J = 9.0$, 2 arom. H); 3.81 (*s*, MeO); 2.29 (*s*, AcS); 1.57, 1.36, 1.32, 1.16 (4*s*, 2 Me_2C). ^{13}C-NMR (75 MHz, $CDCl_3$): see *Table 7*; additionally, 194.66 (*s*, SC=O); 165.84 (*s*, NHC=O); 159.20, 143.36, 143.26 (3*s*); 134.38 (br. *s*, 2 C); 132.91 (*d*); 130.42 (2*d*); 128.78–128.33 (several *d*); 127.70 (2*d*); 114.58, 113.80 (2*s*, 2 Me_2C); 113.64 (2*d*); 88.33 (*s*, Ph_2C); 55.54 (*q*, MeO); 30.74 (*q*, *Me*C=O); 27.33, 27.21, 25.56, 25.38 (4*q*, 2 Me_2C). HR-MALDI-MS: 1108.3442 (15), 1107.3444 (29), 1106.3413 (43, $[M + Na]^+$, $C_{56}H_{57}N_7NaO_{12}S_2^+$; calc. 1106.3404), 273.1280 (100, $MMTr^+$, $C_{20}H_{17}O^+$; calc. 273.1279).

5′-S-Acetyl-2′,3′-O-isopropylidene-5′-thiouridine-6-methyl-(6^1 → 5′-S)-N^6-benzoyl-2′,3′-O-isopropylidene-5′-thioadenosine-8-methyl-(8^1 → 5′-S)-2′,3′-O-isopropylidene-6-{[(4-methoxyphenyl)diphenylmethoxy]methyl}-5′-thiouridine (**17**). Under N_2, a soln. of **16** (300 mg, 0.28 mmol) in O_2-free MeOH (2 ml) was treated with K_2CO_3 (115 mg, 0.83 mmol), and stirred for 10 min at 23°. After dilution with sat. NH_4Cl soln. (20 ml) under N_2, the mixture was extracted with CH_2Cl_2. The combined org. phases were washed with brine, dried ($MgSO_4$), and evaporated. Under N_2, a soln. of the residue (270 mg, 0.26 mmol) in O_2-free DMF (2 ml) was treated with **10** (100 mg, 0.26 mmol) and K_2CO_3 (106 mg, 0.77 mmol), and stirred for 2 h at 23°. The mixture was poured into a sat. NH_4Cl soln. and extracted with CH_2Cl_2. The combined org. phases were washed with brine, dried ($MgSO_4$), and evaporated. FC (CH_2Cl_2/acetone 1:0 → 1:1) gave **17** (150 mg, 42%). R_f (AcOEt/cyclohexane 4:1) 0.20. $[\alpha]^{25}_D = -39.1$ ($c = 1.0$, $CHCl_3$). IR ($CHCl_3$): 3390*w* (br.), 3197*w* (br.), 3015*m*, 2936*w*, 1696*s* (br.), 1612*m*, 1588*w*, 1510*w*, 1457*m*, 1422*w*, 1384*m*, 1354*w*, 1326*w*, 1267*w*, 1254*w* (br.), 1157*w*, 1091*m*, 1070*m*, 1035*w*. ^{1}H-NMR (300 MHz, $CDCl_3$): see *Table 6*; additionally, 10.62, 10.39 (2 br. *s*, H–N(3/I), H–N(3/III)); 10.01 (*s*, HN–C(6/II); 8.04 (*dd*, $J = 6.6$, 3.3, 2 arom. H); 7.47–7.24 (*m*, 15 arom. H); 6.81 (*d*, $J = 8.7$, 2 arom. H); 3.79 (*s*, MeO); 2.29 (*s*, AcS); 1.61, 1.51, 1.38, 1.32 (2 Me), 1.15 (5*s*, 3 Me_2C). ^{13}C-NMR (75 MHz, $CDCl_3$): see *Table 7*; additionally, 194.55 (*s*, SC=O); 165.45 (*s*, NHC=O); 158.81, 142.97 (2 C), 134.05, 133.28 (4*s*); 132.52 (*d*); 130.15 (2*d*); 128.49–128.04 (several *d*); 127.38 (2*d*); 114.48, 113.68, 113.55 (3*s*, 3 Me_2C); 113.36 (2*d*); 88.10 (*s*, Ph_2C); 55.36 (*q*, MeO); 30.68 (*q*, *Me*C=O); 27.27 (2 C), 27.16, 25.43, 25.38 (2 C) (4*q*, 3 Me_2C). HR-MALDI-MS: 1421.423 (16), 1420.419 (54), 1419.417 (97), 1418.420 (100, $[M + Na]^+$, $C_{69}H_{73}NaN_9O_{17}S_3^+$; calc. 1418.418).

N^6-Benzoyl-5′-O-[dimethyl(1,1,2-trimethylpropyl)silyl]-2′,3′-O-isopropylideneadenosine-8-methyl-(8^1 → 5′-S)-2′,3′-O-isopropylidene-5′-thiouridine-6-methyl-(6^1 → 5′-S)-N^6-benzoyl-2′,3′-O-isopropylidene-5′-thioadenosine-8-methyl-(8^1 → 5′-S)-2′,3′-O-isopropylidene-6-{[(4-methoxyphenyl)diphenylmethoxy]methyl}-5′-thiouridine (**18**). Under N_2, a soln. of **17** (150 mg, 0.11 mmol) in O_2-free MeOH (2 ml) was treated with K_2CO_3 (60 mg, 0.43 mmol) and stirred for 10 min at 23°. After dilution with sat. NH_4Cl soln. (20 ml) under N_2, the mixture was extracted with CH_2Cl_2. The combined org. phases were washed with brine, dried ($MgSO_4$), and evaporated. Under N_2, a soln. of the residue (145 mg) in O_2-free DMF (2.5 ml) was treated with **12** (70 mg, 0.11 mmol) and K_2CO_3 (60 mg, 0.43 mmol), and stirred for 2 h at 23°. The mixture was poured into a sat. NH_4Cl soln., and extracted with CH_2Cl_2. The combined org. phases

Table 6. *Selected* ^{1}*H-NMR Chemical Shifts* [ppm] *and Coupling Constants* [Hz] *of the A*[s]U* Dimer* **16**, *the U*[s]A*[s]U* Trimer* **17**, *and the A*[s]U*[s]A*[s]U* Tetramers* **18**–**21**

Solvent	**16**[a]) $CDCl_3$	**17**[b]) $CDCl_3$	**18**[c]) $CDCl_3$	**19**[d]) $CDCl_3$	**20**[e]) $(D_6)DMSO$	**21**[f]) $(D_6)DMSO$
Adenosine unit IV						
H–C(2/IV)			8.70[g])	8.50[g])	8.12[g])	8.11[g])
CH_2–C(8/IV)			4.18–3.95	4.13/4.00[h])	4.13/4.09[h])	4.16–3.97
H–C(1′/IV)			6.32	6.37	6.22	6.18
H–C(2′/IV)			5.86	5.81	5.68	5.61
H–C(3′/IV)			5.15–5.06	5.11	5.05[i])	5.03
H–C(4′/IV)			4.42–4.36	4.32	4.27	4.26
2 H–C(5′/IV)			3.67/3.57	3.58/3.47	3.62–3.45	3.40–3.25
$J(H_a,H_b/IV)$			[m])	14.7	14.5	[m])
J(1′,2′/IV)			2.1	1.8	2.1	2.4
J(2′,3′/IV)			6.0	6.3	6.3	6.3
J(3′,4′/IV)			[m])	4.2	3.0	3.0
J(4′,5′/IV)			6.0/6.3	7.2/6.3	7.0/7.0	[m])
Uridine unit III						
H–C(5/III)		5.09	5.85–5.70	5.72[i])	5.69	5.68
CH_2–C(6/III)		3.58/3.37	3.52/3.36	3.46/3.38	3.62–3.45	3.55–3.40
H–C(1′/III)		5.75	5.85–5.70	5.70	5.74[k])	5.73[h])
H–C(2′/III)		5.22	5.22–5.15	5.18	5.17	5.16
H–C(3′/III)		4.82	5.02–4.94	4.85[k])	4.745[l])	4.76[i])
H–C(4′/III)		3.96	4.28–4.21	4.12–3.90	4.14–4.05	4.06
2 H–C(5′/III)		3.21/3.16	2.92–2.72	3.03–2.72	2.85–2.81	2.90–2.67
$J(H_a,H_b/III)$		15.0	14.5	14.7	[m])	[m])
J(1′,2′/III)		< 1.5	[m])	< 1.5	< 1.5	< 1.5
J(2′,3′/III)		6.3	[m])	6.3	6.2	6.3
J(3′,4′/III)		3.9	[m])	3.3	3.7	< 1.5
J(4′,5′/III)		6.6/7.2	[m])	[m])	[m])	[m])
Adenosine unit II						
H–C(2/II)	8.75	8.74	8.71[g])	8.33[g])	8.15[g])	8.14[g])
CH_2–C(8/II)	3.67/3.49	3.90–3.65	4.18–3.95	4.11/4.00[h])	4.07/4.01[h])	4.16–3.97
H–C(1′/II)	6.16	6.22	6.22	6.32	6.25	6.21
H–C(2′/II)	5.82	5.62	5.85–5.70	5.96	5.78	5.67
H–C(3′/II)	5.06	5.21	5.15–5.06	5.11	5.03[i])	5.03
H–C(4′/II)	4.28	4.41	4.28–4.21	4.21	4.14–4.05	4.12
2 H–C(5′/II)	3.19/3.07	2.84–2.72	2.92–2.72	3.03–2.72	2.85–2.81	2.90–2.67
$J(H_a,H_b/II)$	12.3	[m])	[m])	14.7	14.5	[m])
J (1′,2′/II)	2.1	< 1.5	< 1.5	1.5	1.7	1.8
J (2′,3′/II)	6.3	6.0	[m])	6.3	6.2	6.3
J (3′,4′/II)	3.0	3.9	[m])	3.0	3.3	3.0
J (4′,5′/II)	7.5/6.9	6.3/6.3	[m])	6.6/6.6	[m])	[m])
Uridine unit I						
H–C(5/I)	5.39	5.44	5.85–5.70	5.35[i])	5.63	5.62
CH_2–C(6/I)	4.06/4.00	4.16–4.02	4.18–3.95	4.12–3.90	4.36/4.32	4.38–4.28
H–C(1′/I)	5.39	5.53	5.85–5.70	5.70	5.73[k])	5.71[h])
H–C(2′/I)	4.81	4.91	5.02–4.94	5.18	5.17	5.16
H–C(3′/I)	4.68	4.53	4.68–4.60	4.82[k])	4.740[l])	4.72[i])
H–C(4′/I)	3.99	4.14–4.04	4.18–4.11	4.12–3.90	4.14–4.05	4.06

Table 6 (cont.)

Solvent	**16**[a]) $CDCl_3$	**17**[b]) $CDCl_3$	**18**[c]) $CDCl_3$	**19**[d]) $CDCl_3$	**20**[e]) $(D_6)DMSO$	**21**[f]) $(D_6)DMSO$
2 H–C(5′/I)	2.82–2.65	2.84–2.72	2.92–2.72	3.03–2.72	2.87/2.74	2.90–2.67
$J(H_a,H_b/I)$	14.7	[m])	[m])	[m])	14.8	[m])
$J(1',2'/I)$	1.8	< 2	[m])	< 1.5	< 1.5	< 1.5
$J(2',3'/I)$	6.3	6.0	[m])	6.3	6.2	6.3
$J(3',4'/I)$	3.9	4.2	[m])	3.3	3.7	< 1.5
$J(4',5'/I)$	8.1/3.9	[m])	[m])	[m])	7.7/6.4	[m])

[a]) $J(5'a,5'b/II) = 13.8$ Hz. [b]) Broad signals for H–C(5/III), CH_2–C(8/II), and all H-atoms of unit I. $J(5'a,5'b/III) = 13.5$ Hz. [c]) Broad signals. $J(5'a,5'b/IV) = 12.6$ Hz. [d]). Broad signals for CH_2–C(8/II). $J(5'a,5'b/IV) = 10.5$ Hz. [e]) $J(5'a,5'b/I) = 13.7$, $J(H_a,OH/I) = 6.0$, $J(H_b,OH/I) = 5.1$ Hz. [f]) Assignments based on a HSQC and a HMBC spectrum. [g])–[l]) Assignments may be interchanged. [m]) Not assigned.

were washed with brine, dried ($MgSO_4$), and evaporated. FC (CH_2Cl_2/MeOH/NH_4OH 98:2:1 → 90:10:1) gave **18** (90 mg, 44%). R_f (CH_2Cl_2/MeOH 95:5) 0.38. $[\alpha]^{25}_D = -44.9$ ($c = 1.0$, $CHCl_3$). IR ($CHCl_3$): 3396*w* (br.), 3204*w* (br.), 3015*m*, 2959*w*, 2933*w*, 2869*w*, 1698*s* (br.), 1612*s*, 1589*m*, 1511*w*, 1458*m*, 1423*m*, 1384*m*, 1357*m*, 1330*w*, 1263*m*, 1243*m*, 1157*w*, 1089*s* (br.). ^{1}H-NMR (300 MHz, $CDCl_3$): see *Table 6*; additionally, 10.2, 9.73 (2 br. *s*, H–N(3/I), H–N(3III)); 9.55 (*s*, HN–C(6/II), HN–C(6/IV)); 8.02–7.92 (*m*, 4 arom. H); 7.53–7.24 (*m*, 18 arom. H); 6.82 (*d*, $J = 9.0$, 2 arom. H); 3.79 (*s*, MeO); 1.60 (2 Me), 1.46, 1.39 (2 Me), 1.33, 1.27, 1.16 (6*s*, 4 Me_2C); 1.50–1.40 (*m*, Me_2CH); 0.82 (*d*, $J = 6.9$, Me_2CH); 0.78, 0.77 (2*s*, Me_2CSi); −0.03, −0.04 (2*s*, Me_2Si). ^{13}C-NMR (75 MHz, $CDCl_3$): see *Table 7*; additionally, 166.10, 165.86 (2*s*, 2 NHC=O); 159.24, 143.38, 143.30 (3*s*); 134.35 (2*s*); 134.30 (*s*); 132.84, 132.72 (2*d*); 130.55 (2*d*); 128.86–128.34 (several *d*); 127.67 (2*d*); 114.79, 114.32, 114.06, 113.92 (4*s*, 4 Me_2C); 113.65 (2*d*); 88.45 (*s*, Ph_2C); 55.50 (*q*, MeO); 34.28 (*d*, Me_2CH); 27.41 (br. *q*, 4 C), 25.64 (*q*), 25.53 (br. *q*, 3 C) (4 Me_2C); 25.53 (*s*, Me_2CSi); 20.49 (*q*, Me_2CH); 18.67 (*q*, Me_2CSi); −3.25 (*q*, Me_2Si). HR-MALDI-MS: 1943.687 (68), 1942.684 (100), 1941.682 (80, $[M + Na]^+$, $C_{96}H_{110}N_{14}NaO_{21}S_3Si^+$; calc. 1941.683).

5′-O-[Dimethyl(1,1,2-trimethylpropyl)silyl]-2′,3′-O-isopropylideneadenosine-8-methyl-(8^1 → 5′-S)-2′,3′-O-isopropylidene-5′-thiouridine-6-methyl-(6^1 → 5′-S)-2′,3′-O-isopropylidene-5′-thioadenosine-8-methyl-(8^1 → 5′-S)-2′,3′-O-isopropylidene-6-{[(4-methoxyphenyl)diphenylmethoxy]methyl}-5′-thiouridine (**19**). A soln. of **18** (90 mg, 47 µmol) in MeOH (2 ml) was treated with MeONa (25 mg, 0.47 mmol) and stirred for 12 h at 23°. The mixture was poured into sat. NH_4Cl soln. and extracted with CH_2Cl_2. The combined org. phases were washed with brine, dried ($MgSO_4$), and evaporated. FC (AcOEt/acetone/NH_4OH 100:0:1 → 50:50:1) gave **19** (52 mg, 65%). R_f (CH_2Cl_2/MeOH 92:5) 0.55. $[\alpha]^{25}_D = -97.9$ ($c = 1.0$, $CHCl_3$). IR ($CHCl_3$): 3314*w*, 3200*w*, 1698*s*, 1641*m*, 1510*w*, 1459*w*, 1441*w*, 1375*m*, 1330*w*, 1299*w*, 1208*w*, 1157*m*, 1092*s*. ^{1}H-NMR (300 MHz, $CDCl_3$): see *Table 7*; additionally, 13.03, 12.38 (2 br. *s*, H–N(3/I), H–N(3/III)); 7.66 (br. *s*, NH_2); 7.48–7.28 (*m*, 12 arom. H, NH_2); 6.85 (*d*, $J = 8.7$, 2 arom. H); 3.80 (*s*, MeO); 1.62, 1.59, 1.47, 1.42, 1.40, 1.39, 1.28, 1.23 (8*s*, 4 Me_2C); 1.53 (*sept.*, $J = 6.9$, Me_2CH); 0.81 (*d*, $J = 6.9$, Me_2CH); 0.76, 0.75 (2*s*, Me_2CSi); −0.03, −0.06 (2*s*, Me_2Si). ^{13}C-NMR (75 MHz, $CDCl_3$): see *Table 7*; additionally, 158.86, 143.18, 142.99, 134.05 (4*s*); 130.33 (2*d*); 128.19 (4*d*); 128.04 (4*d*); 127.35 (2*d*); 113.55, 113.47 (br., 3 C) (2*s*, 4 Me_2C); 113.36 (2*d*); 88.27 (*s*, Ph_2C); 55.33 (*q*, MeO); 34.27 (*d*, Me_2CH); 27.34, 27.28 (2 C), 27.18, 25.72, 25.59, 25.28 (2 C) (6*q*, 4 Me_2C); 25.28 (*s*, Me_2CSi); 20.40 (*q*, Me_2CH); 18.58 (*q*, Me_2CSi); −3.29 (*q*, Me_2Si). HR-MALDI-MS: 1735.634 (62), 1734.631 (96), 1733.629 (100, $[M + Na]^+$; $C_{82}H_{102}N_{14}NaO_{19}S_3Si^+$: calc. 1733.628).

5′-O-[Dimethyl(1,1,2-trimethylpropyl)silyl]-2′,3′-O-isopropylideneadenosine-8-methyl-(8^1 → 5′-S)-2′,3′-O-isopropylidene-5′-thiouridine-6-methyl-(6^1 → 5′-S)-2′,3′-O-isopropylidene-5′-thioadenosine-8-methyl-(8^1 → 5′-S)-6-(hydroxymethyl)-2′,3′-O-isopropylidene-5′-thiouridine (**20**). Under N_2, a soln. of **19** (30 mg, 18 µmol) in CH_2Cl_2 (1 ml) was treated with Cl_2CHCO_2H (50 µl, 0.6 mmol) and Et_3SiH (10 µl ,

Table 7. *Selected ^{13}C-NMR Chemical Shifts* [ppm] *of the A*[s]U* Dimer* **16**, *the U*[s]A*[s]U* Trimer* **17**, *and the A*[s]U*[s]A*[s]U* Tetramers* **18**–**21**

Solvent	**16** $CDCl_3$	**17** $CDCl_3$	**18** $CDCl_3$	**19** $CDCl_3$	**20** $(D_6)DMSO$	**21**[a]) $(D_6)DMSO$
Adenosine unit IV						
C(2/IV)			152.41	153.12[b])	152.25	152.25
C(4/IV)			149.89	150.46[c])	149.66[b])	149.64[b])
C(5/IV)			122.14	118.26[d])	117.78	117.78
C(6/IV)			152.65	155.75[e])	155.51[c])	155.50
C(8/IV)			152.18[b])	149.46[c])	148.08	147.87
CH_2–C(8/IV)			27.90	29.81	28.89	27.04
C(1′/IV)			87.83	89.02[f])	88.89	89.09
C(2′/IV)			83.27	83.17	82.45[d])	82.22[c])
C(3′/IV)			81.87	82.98[g])	81.47	81.17
C(4′/IV)			85.07	88.02	85.57	85.53
C(5′/IV)			62.91	62.88	62.58	61.30
Uridine unit III						
C(2/III)		151.71[b])	152.06[b])	152.53[h])	150.72[e])	150.70[d])
C(4/III)		162.62	162.24	[m])	161.92	161.92
C(5/III)		103.23[c])	104.12[c])	104.06	103.43	103.42
C(6/III)		151.16[b])	151.28[b])	151.33[i])	151.14	151.15
CH_2–C(6/III)		33.00[d])	33.48[d])	32.90[k])	31.64	31.82
C(1′/III)		91.44	91.32	[m])	90.44	90.42
C(2′/III)		84.44[e])	83.95	85.27[l])	84.18[f])	84.18[e])
C(3′/III)		84.24[e])	83.95	84.83	83.70[g])	83.35
C(4′/III)		89.40	89.81	89.41	87.45[h])	87.45[f])
C(5′/III)		32.62[d])	33.28[d])	34.15[k])	33.53[i])	33.28
Adenosine unit II						
C(2/II)	152.53	152.46	152.41	152.61[b])	152.46	152.46
C(4/II)	149.38	149.64	149.32	150.46[c])	149.71[b])	149.71[b])
C(5/II)	122.32	123.22	122.14	118.40[d])	117.78	117.78
C(6/II)	152.94	152.46[b])	152.65	155.40[e])	155.48[c])	155.50
C(8/II)	151.66[b])	150.79	151.21[b])	150.28[c])	147.89	147.87
CH_2–C(8/II)	31.37	31.48	27.90	29.81	28.89	27.04
C(1′/II)	87.96	88.10	88.00	88.53[f])	88.81	88.80
C(2′/II)	83.74	83.77[e])	83.95	83.17	82.64[d])	82.62[c])
C(3′/II)	84.20	84.03[e])	83.27	82.20[g])	83.73	83.68
C(4′/II)	86.87	87.51	87.83	88.02	87.06	86.26
C(5′/II)	33.55	33.00[d])	33.28[d])	32.90[k])	32.61[i])	33.28
Uridine unit I						
C(2/I)	152.53 [b])	152.08[b])	152.06[b])	152.53[h])	150.79[e])	150.79[d])
C(4/I)	163.41	163.08	163.05	163.05	162.64	162.64
C(5/I)	103.71	103.86[c])	103.48[c])	104.06	100.86	100.85
C(6/I)	151.66[b])	150.95[b])	151.09[b])	151.33[i])	154.84	154.83
CH_2–C(6/I)	62.53	62.34	62.57	62.88	59.25	59.24
C(1′/I)	92.63	92.07	92.14	[m])	90.80	90.81
C(2′/I)	84.82	85.01[e])	84.71	85.07[l])	84.40[f])	84.40[e])
C(3′/I)	84.82	84.44[e])	84.52	84.83	83.35[g])	83.35
C(4′/I)	90.42	89.66	90.14	89.41	87.64[h])	87.57[f])
C(5′/I)	33.55	33.78[d])	32.80[d])	34.15[k])	33.23[i])	33.28

[a]) Assignments based on a HSQC and a HMBC spectrum. [b])–[l]) Assignments may be interchanged. [m]) Hidden by the noise.

63 μmol), and stirred for 10 min at 23°. The mixture was poured into sat. $NaHCO_3$ soln. and extracted with CH_2Cl_2. The combined org. phases were washed with brine, dried ($MgSO_4$), and evaporated. Trituration of the crude material in cyclohexane, followed by FC (CH_2Cl_2/MeOH/NH_4OH 95:5:1 → 90:10:1), gave **20** (6 mg, 24%). R_f (CH_2Cl_2/MeOH 9:1) 0.30. $[\alpha]^{25}_D = -86.5$ ($c = 1.0$, $CHCl_3$). UV 263 (31625). IR ($CHCl_3$): 3472*w* (br.), 3389*w* (br.), 3327*w* (br.), 3195*w* (br.), 2971*m*, 2931*m*, 1696*s* (br.), 1643*m*, 1604*m*, 1522*w*, 1478*w*, 1425*m*, 1386*m*, 1376*m*, 1331*w*, 1298*w*, 1157*m*, 1089*s*, 1046*m*. ^{1}H-NMR (500 MHz, (D_6)DMSO): see *Table 6*; additionally, 11.40 (br. *s*, H–N(3/I), H–N(3/III)); 7.25 (br. *s*, 2 NH_2); 5.84 (*t*, $J = 5.5$, *H*OCH_2–C(6/I)); 1.54, 1.53, 1.41, 1.39, 1.32, 1.31, 1.24, 1.23 (8*s*, 4 Me_2CO_2); 1.47 (*sept.*, $J = 6.8$, Me_2C*H*); 0.770, 0.768 (2*d*, $J = 6.8$, *Me*$_2$CH); 0.72, 0.71 (2*s*, Me_2CSi); −0.10, −0.11 (2*s*, Me_2Si). ^{13}C-NMR (125 MHz, (D_6)DMSO): see *Table 7*; additionally, 113.27, 112.87, 112.48, 112.47 (4*s*, 4 Me_2*C*); 33.54 (*d*, Me_2*C*H); 26.87 (2 C), 26.80, 25.13, 25.06, 24.96, 24.89, 24.60 (7*q*, 4 *Me*$_2$C); 25.54 (*s*, Me_2*C*Si); 20.03, 20.00 (2*q*, *Me*$_2$CH); 18.19, 18.16 (2*q*, *Me*$_2$CSi); −3.71, −3.75 (2*q*, Me_2Si). HR-MALDI-MS: 1480.474 (34), 1479.481 (62), 1478.483 (86), 1477.476 (100, $[M+K]^+$, $C_{62}H_{86}KN_{14}O_{18}S_3Si^+$; calc. 1477.481), 1464.499 (31), 1463.503 (51), 1462.507 (70), 1461.505 (86, $[M+Na]^+$, $C_{62}H_{86}N_{14}NaO_{18}S_3Si^+$; calc. 1461.507).

*2′,3′-*O*-Isopropylideneadenosine-8-methyl-(8^1 → 5′-*S*)-2′,3′-*O*-isopropylidene-5′-thiouridine-6-methyl-(6^1 → 5′-*S*)-2′,3′-*O*-isopropylidene-5′-thioadenosine-8-methyl-(8^1 → 5′-*S*)-6-(hydroxymethyl)-2′,3′-*O*-isopropylidene-5′-thiouridine* (**21**). Under N_2, a soln. of **20** (60 mg, 30 μmol) in THF (1 ml) was treated with $(HF)_3 \cdot Et_3N$ (50 μl, 0.3 mmol) and stirred for 3 d at 23°. The mixture was poured into sat. $NaHCO_3$ soln. and extracted with CH_2Cl_2. The combined org. phases were washed with brine, dried ($MgSO_4$), and evaporated. The crude material was purified by repeated trituration with hexane and AcOEt to yield **21** (15 mg, 38%). R_f (CH_2Cl_2/MeOH 92:8) 0.37. $[\alpha]^{25}_D = -41.8$ ($c = 1.0$, $CHCl_3$). UV 263 (48259). IR ($CHCl_3$): 3527*w*, 3472*w*, 3408*w*, 3319*w*, 3200*w*, 3019*s*, 2962*w*, 2928*w*, 1710*m*, 1682*m*, 1644*w*, 1603*w*, 1455*w*, 1304*w*, 1276*w*, 1262*m*, 1221*s*, 1093*m*, 1011*m*. ^{1}H-NMR (300 MHz, (D_6)DMSO; assignments based on a HSQC and a HMBC spectrum): see *Table 6*; additionally, 11.41 (br. *s*, H–N(3/I and III)); 7.32, 7.29 (2 br. *s*, 2 NH_2); 7.3–7.1 (br. *s*, HO–C(5′/IV)); 5.90–5.78 (br. *s*, *H*OCH_2–C(6/I)); 1.54 (2 Me), 1.39, 1.31 (2 Me), 1.28, 1.23 (2 Me) (5*s*, 4 Me_2C). ^{13}C-NMR (150 MHz, (D_6)DMSO; assignments based on a HSQC and a HMBC spectrum): see *Table 7*; additionally, 113.25, 113.08, 112.47 (2 C) (3*s*, 4 Me_2*C*); 26.85, 26.83, 26.49, 26.45, 25.18, 25.04, 24.94, 24.87 (8*q*, 4 *Me*$_2$C). HR-MALDI-MS: 1322.392 (16), 1321.391 (38), 1320.392 (67), 1319.389 (100, $[M+Na]^+$, $C_{54}H_{68}N_{14}NaO_{18}S_3^+$; calc. 1319.390).

*5′-*S*-Acetyl-2′,3′-*O*-isopropylidene-5′-thiouridine-6-methyl-(6^1 → 5′-*S*)-*N*^{6}-benzoyl-2′,3′-*O*-isopropylidene-8-{[(4-methoxyphenyl)diphenylmethoxy]methyl}-5′-thioadenosine* (**22**). Under N_2, a soln. of **13** (410 mg, 0.53 mmol) in O_2-free MeOH (2 ml) was treated with freshly powdered K_2CO_3 (220 mg, 1.55 mmol) and stirred for 10 min at 23°. After dilution with sat. NH_4Cl soln. (20 ml), the mixture was extracted with CH_2Cl_2. The combined org. phases were washed with brine, dried ($MgSO_4$), and evaporated. Under N_2, a soln. of the residue (380 mg) in O_2-free DMF (2 ml) was treated with **10** (203 mg, 0.52 mmol) and K_2CO_3 (118 mg, 0.85 mmol), and stirred for 2 h at 23°. The mixture was poured into sat. NH_4Cl soln. and extracted with CH_2Cl_2. The combined org. phases were washed with brine, dried ($MgSO_4$), and evaporated to yield **22** (530 mg, 94%) that was directly used for the next step. For analysis, a sample was purified by FC (AcOEt/cyclohexane 3:2 → 1:0). R_f (AcOEt/cyclohexane 4:1) 0.35. $[\alpha]^{25}_D = -34.3$ ($c = 1.0$, $CHCl_3$). IR ($CHCl_3$): 3395*w* (br.), 3204*w* (br.), 3016*m*, 1697*s* (br.), 1614*m*, 1588*w*, 1510*m*, 1489*w*, 1448*m*, 1428*m*, 1384*m*, 1372*w*, 1356*w*, 1299*w*, 1259*m*, 1243*m*, 1157*w*, 1090*m*, 1070*m*, 1037*w*. ^{1}H-NMR (300 MHz, $CDCl_3$): see *Table 8*; additionally, 11.96 (br. *s*, H–N(3/II)); 10.55 (br. *s*, HN–C(6/I)); 8.15–8.01 (*m*, 2 arom. H); 7.52–7.21 (*m*, 15 arom. H); 6.85–6.79 (*m*, 2 arom. H); 3.75 (*s*, MeO); 2.25 (*s*, AcS); 1.57, 1.52, 1.35 (2 Me) (3*s*, 2 Me_2C). ^{13}C-NMR (75 MHz, $CDCl_3$): see *Table 9*; additionally, 194.49 (*s*, SC=O); 165.12 (*s*, NHC=O); 158.68, 143.39, 143.09, 134.11, 132.03 (5*s*); 132.30 (*d*); 130.35 (2*d*); 128.56–127.98 (several *d*); 127.23, 127.15 (2*d*); 114.36, 113.49 (2*s*, 2 Me_2*C*); 113.36 (2*d*); 88.15 (*s*, Ph_2*C*); 55.23 (*q*, MeO); 30.57 (*q*, *Me*C=O); 27.37, 27.22, 25.47, 25.33 (4*q*, 2 *Me*$_2$C). HR-MALDI-MS: 1108.362 (19), 1107.357 (50), 1106.353 (68, $[M+Na]^+$, $C_{56}H_{58}N_7NaO_{12}S_2^+$; calc. 1106.340), 1086.370 (29), 1085.365 (66), 1084.359 (100, $[M+H]^+$, $C_{56}H_{59}N_7O_{12}S_2^+$; calc. 1084.358).

*5′-*S*-Acetyl-*N*^{6}-benzoyl-2′,3′-*O*-isopropylidene-5′-thioadenosine-8-methyl-(8^1 → 5′-*S*)-2′,3′-*O*-isopropylidene-5′-thiouridine-6-methyl-(6^1 → 5′-*S*)-*N*^{6}-benzoyl-2′,3′-*O*-isopropylidene-8-{[(4-methoxyphenyl)-diphenylmethoxy]methyl}-5′-thioadenosine* (**23**). Under N_2, a soln. of **22** (110 mg, 0.1 mmol) in O_2-free

Table 8. *Selected* ^{1}*H-NMR Chemical Shifts* [ppm] *and Coupling Constants* [Hz] *of the U*[s]A* Dimer* **22**, *the A*[s]U*[s]A* Trimer* **23**, *and the U*[s]A*[s]U*[s]A* Tetramers* **24**–**27**

Solvent	**22** $CDCl_3$	**23**[a]) $CDCl_3$	**24** $(D_6)DMSO$	**25** $(D_6)DMSO$	**26**[b]) $CDCl_3$ (2°)	**27**[c]) $(D_6)DMSO$
Uridine unit IV						
H–C(5/IV)			5.59[d])	5.63[d])	5.87	5.64[d])
CH_2–C(6/IV)			3.79–3.60	3.78–3.60	3.85/3.11	3.70–3.65
H–C(1′/IV)			5.76[e])	5.71[e])	5.23	5.46
H–C(2′/IV)			5.18	5.17	5.11	4.50
H–C(3′/IV)			4.73	4.75–4.63	4.92	4.10–4.06
H–C(4′/IV)			4.08–3.98	4.10–3.92	3.90	3.70
2 H–C(5′/IV)			4.32–4.23	4.32–4.20	3.91/3.44	3.59/3.43
$J(H_a,H_b/IV)$			[h])	[h])	16.8	[h])
J(1′,2′/IV)			< 1.5	< 1.5	[h])	3.7
J(2′,3′/IV)			6.3	6.0	6.0	[h])
J(3′,4′/IV)			3.9	[h])	2.4	6.6
J(4′,5′/IV)			[h])	[h])	[h])	3.4/5.4
Adenosine unit III						
H–C(2/III)		8.71	8.13[f])	8.13[f])	7.94	8.13
CH_2–C(8/III)		4.07–3.94	3.79–3.60	3.78–3.60	4.07/3.64	4.06–4.02
H–C(1′/III)		6.25	6.20	6.20	6.31	5.87
H–C(2′/III)		5.78	5.66	5.64	5.20	5.08
H–C(3′/III)		5.06	5.02	5.01[g])	5.13	4.31
H–C(4′/III)		4.24	4.24–4.15	4.10–3.92	4.48	4.06–4.02
2 H–C(5′/III)		3.10/3.00	2.94–2.68	2.72–2.64	3.40/2.54	3.02/2.91
$J(H_a,H_b/III)$		[h])	[h])	[h])	14.9	[h])
J(1′,2′/III)		1.5	1.5	1.8	[h])	5.2
J(2′,3′/III)		6.3	6.3	6.3	6.0	[h])
J(3′,4′/III)		3.3	3.0	3.0	[h])	[h])
J(4′,5′/III)		7.5/6.9	[h])	[h])	10.8/[h])	5.1/4.8
Uridine unit II						
H–C(5/II)	4.92	5.09	5.63[d])	5.62[d])	4.77	5.63[d])
CH_2–C(6/II)	3.73/3.32	3.59/3.34	3.79–3.60	3.78–3.60	4.05/3.48	3.70–3.65
H–C(1′/II)	5.74	5.68	5.71[e])	5.75[e])	6.06	5.43
H–C(2′/II)	5.29	5.16	5.15	5.14	5.49	4.56
H–C(3′/II)	4.84	4.87	4.71	4.75–4.63	4.87	4.17
H–C(4′/II)	4.06	4.11	4.08–3.98	4.10–3.92	4.41	3.86
2 H–C(5′/II)	3.25–3.01	2.93–2.79	2.94–2.68	2.72–2.64	2.58/2.45	2.91/2.79
$J(H_a,H_b/II)$	14.7	15.0	[h])	[h])	13.2	[h])
J (1′,2′/II)	< 1.5	< 1.5	< 1.5	< 1.5	[h])	3.2
J (2′,3′/II)	6.3	6.3	6.6	6.0	6.0	[h])
J (3′,4′/II)	3.9	4.2	3.9	[h])	[h])	6.3
J (4′,5′/II)	6.9/6.9	7.2/7.2	[h])	[h])	10.2/[h])	5.6/7.1
Adenosine unit I						
H–C(2/I)	8.77	8.74	8.17[f])	8.14[f])	8.38	8.15
CH_2–C(8/I)	4.79/4.50	4.65/4.49	4.11/3.97	4.75–4.63	5.07/4.96	4.70/4.65
H–C(1′/I)	6.23	6.22	5.97	6.31	6.63	6.02
H–C(2′/I)	5.37	5.44	5.60	5.57	5.05	5.08
H–C(3′/I)	5.23	5.11	4.85	5.00[g])	5.41	4.31
H–C(4′/I)	4.46	4.34	4.24–4.15	4.10–3.92	4.65	4.06–4.02

Table 8 (cont.)

Solvent	**22** $CDCl_3$	**23**[a]) $CDCl_3$	**24** $(D_6)DMSO$	**25** $(D_6)DMSO$	**26**[b]) $CDCl_3$ (2°)	**27**[c]) $(D_6)DMSO$
2 H–C(5′/I)	3.25–3.01	2.93–2.79	2.94–2.68	2.72–2.64	3.52/2.85	3.02/2.91
$J(H_a,H_b/I)$	12.3	12.0	14.4	[h])	11.4	13.1
$J(1',2'/I)$	< 1.5	1.8	2.7	2.1	[h])	5.3
$J(2',3'/I)$	6.3	6.6	6.3	6.3	6.0	[h])
$J(3',4'/I)$	4.8	4.2	3.0	3.0	4.8	[h])
$J(4',5'/I)$	[h])	7.8/4.2	[h])	[h])	10.2/[h])	5.1/4.8

[a]) $J(5'a,5'b/III) = 13.5$ Hz. [b]) At 600 MHz. Broad signals with the exception of H–C(4/I) (couplings smaller than 2 Hz not visible). Assignment based on DQFCOSY, TOCSY, and NOESY spectra. $J(5'a,5'b/I) = 15.8$, $J(5'a,5'b/II) = 13.8$, $J(5'a,5'b/III) = 15.3$, $J(5'a,5'b/IV) = 12.3$ Hz. [c]) At 500 MHz. Assignments based on DQFCOSY, HSQC, and HMBC spectra. Broad CHOH and CH_2OH signals due to $^3J(H,OH)$ couplings. $^4J(5,NH/II) = {}^4J(5,NH/IV) = 2.1$, $J(5'a,5'b/I) = J(5'a,5'b/III) = 13.6$, $J(5'a,5'b/II) = 13.5$, $J(5'a,5'b/IV) = 11.8$ Hz. [d])–[g]) Assignments may be interchanged. [h]) Not assigned.

MeOH (1 ml) was treated with freshly powdered K_2CO_3 (42 mg, 0.3 mmol), and stirred for 10 min at 23°. After dilution with sat. NH_4Cl soln. (20 ml) under N_2, the mixture was extracted with CH_2Cl_2. The combined org. phases were washed with brine, dried ($MgSO_4$), and evaporated. Under N_2, a soln. of the residue (100 mg) in O_2-free DMF (1 ml) was treated with **12** (49 mg, 96 μmol) and K_2CO_3 (53 mg, 0.38 mmol), and stirred for 2 h at 23°. The mixture was poured into sat. NH_4Cl soln. and extracted with CH_2Cl_2. The combined org. phases were washed with brine, dried ($MgSO_4$), and evaporated to yield **23** (150 mg, > 98%) that was directly used for the next step. For analysis, a sample was purified by FC (AcOEt/cyclohexane 3 : 2 → 1 : 0). R_f (AcOEt) 0.53. $[\alpha]^{25}_D = -32.5$ ($c = 1.0$, $CHCl_3$). IR ($CHCl_3$): 3404*w* (br.), 3211*w* (br.), 3015*m*, 2928*m*, 2855*w*, 1698*s* (br.), 1613*s*, 1589*m*, 1510*w*, 1458*m*, 1448*m*, 1425*m*, 1384*m*, 1376*m*, 1356*m*, 1267*m*, 1090*s*. ^{1}H-NMR (300 MHz, $CDCl_3$): see *Table 8*; additionally, 10.4 (br. *s*, H–N(3/II); 9.78 (br. *s*), 9.34 (*s*) (HN–C(6/I), HN–C(6/III)); 8.06–8.00 (*m*, 2 arom. H); 7.92–7.90 (*m*, 2 arom. H); 7.52–7.19 (*m*, 18 arom. H); 6.84–6.79 (*m*, 2 arom. H); 3.74 (*s*, MeO); 2.27 (*s*, AcS); 1.56, 1.53, 1.46, 1.36, 1.35, 1.27 (6*s*, 3 Me_2C). ^{13}C-NMR (75 MHz, $CDCl_3$): see *Table 9*; additionally, 194.14 (*s*, SC=O); 165.01 162.44 (2*s*, 2 NHC=O); 158.69, 143.35, 143.13 (3*s*); 134.06 (2*s*); 133.62 (*s*); 132.43 (2*d*); 130.38 (2*d*); 128.54–127.94 (several *d*); 127.21, 127.15 (2*d*); 114.48, 114.12, 113.58 (3*s*, 3 Me_2C); 113.33 (2*d*); 88.11 (*s*, Ph_2C); 55.24 (*q*, MeO); 30.56 (*q*, *Me*C=O); 27.34, 27.19, 27.13, 25.50, 25.38, 25.30 (6*q*, 3 Me_2C). HR-ESI-MS: 1547.479 (12), 1546.475 (26), 1545.473 (27, $[M+Na]^+$, $C_{77}H_{78}N_{12}NaO_{16}S_3^+$; calc. 1545.472), 1525.478 (8), 1524.471 (20), 1523.470 (27, $[M+H]^+$, $C_{77}H_{79}N_{12}O_{16}S_3^+$; calc. 1523.490), 774.230 (16), 773.728 (27), 773.227 (29, $[M+Na+H]^{2+}$, $C_{77}H_{79}N_{12}NaO_{16}S_3^{2+}$; calc. 773.240), 763.738 (26), 763.235 (58), 762.734 (96), 762.235 (100, $[M+2H]^{2+}$, $C_{77}H_{80}N_{12}O_{16}S_3^{2+}$; calc. 762.249).

*5′-*O*-[Dimethyl(1,1,2-trimethylpropyl)silyl]-2′,3′-*O*-isopropylideneuridine-6-methyl-(6¹ → 5′-*S*)-2′,3′-*O*-isopropylidene-5′-thioadenosine-8-methyl-(8¹ → 5′-*S*)-2′,3′-*O*-isopropylidene-5′-thiouridine-6-methyl-(6¹ → 5′-*S*)-2′,3′-*O*-isopropylidene-8-{[(4-methoxyphenyl)diphenylmethoxy]methyl}-5′-thioadenosine* (**24**). Under N_2, a soln. of **23** (125 mg, 82 μmol) in O_2-free MeOH (1 ml) was treated with K_2CO_3 (45 mg, 0.33 mmol), and stirred for 10 min at 23°. MeOH was evaporated under N_2. A soln. of the residue in O_2-free DMF (1 ml) was treated with **7** (39 mg, 82 μmol), and stirred for 2 h at 23°. The mixture was poured into sat. NH_4Cl soln. and extracted with CH_2Cl_2. The combined org. phases were washed with brine, dried ($MgSO_4$), and evaporated. A soln. of the residue in MeOH (2 ml) was treated with MeONa (44 mg, 0.82 mmol) and stirred for 12 h at 23°. The mixture was poured on sat. NH_4Cl soln. and extracted with CH_2Cl_2. The combined org. phases were washed with brine, dried ($MgSO_4$), and evaporated. FC (CH_2Cl_2/MeOH/NH_4OH 95 : 5 : 1 → 90 : 10 : 1) gave **24** (40 mg, 28%). R_f (AcOEt/MeOH 92 : 8) 0.64. $[\alpha]^{25}_D = -35.5$ ($c = 1.1$, $CHCl_3$). IR ($CHCl_3$): 3479*w*, 3390*w* (br.), 3325*w*, 3192*w*, 2996*s*, 2965*m*, 2934*m*, 2866*w*, 1697*s* (br.), 1640*s*, 1606*m*, 1510*w*, 1448*m*, 1377*s*, 1330*m*, 1299*m*, 1263*m*, 1243*m* (br.), 1157*m*, 1056*s*,

Table 9. *Selected ^{13}C-NMR Chemical Shifts* [ppm] *of the U*[s]A* Dimer* **22**, *the A*[s]U*[s]A* Trimer* **23**, *and the U*[s]A*[s]U*[s]A* Tetramers* **25**–**27**

Solvent	**22** $CDCl_3$	**23** $CDCl_3$	**25** $(D_6)DMSO$	**26** $CDCl_3$	**27**[a]) $(D_6)DMSO$
Uridine unit IV					
C(2/IV)			150.99[b])	151.41	150.60
C(4/IV)			161.75[c])	161.9	162.02
C(5/IV)			103.35	103.7	103.13
C(6/IV)			152.43[d])	152.27	152.16[b])
CH_2–C(6/IV)			32.63	32.78[b])	32.21
C(1′/IV)			90.76	91.56	91.71
C(2′/IV)			84.39[e])	85.26[c])	71.27
C(3′/IV)			81.87	80.25	69.59
C(4′/IV)			87.54	91.03	84.70
C(5′/IV)			63.59	62.19	61.83
Adenosine unit III					
C(2/III)		151.11	150.73	150.59	152.01
C(4/III)		149.00	149.52	149.71	149.97
C(5/III)		121.98	117.45	117.8	117.79
C(6/III)		152.06[b])	155.34	155.03	155.25
C(8/III)		151.76[b])	147.73	148.65	148.73
CH_2–C(8/III)		31.16	31.68	30.06	27.78
C(1′/III)		89.62[c])	88.78	90.11	88.77
C(2′/III)		84.05[d])	82.86[e])	84.52[c])	71.15[c])
C(3′/III)		83.88[d])	83.75[e])	85.14[c])	72.50[d])
C(4′/III)		86.68	85.46	89.66	83.28[e])
C(5′/III)		32.05[e])	33.66	32.72[b])	33.23
Uridine unit II					
C(2/II)	152.63[b])	152.43	150.65[b])	151.41	150.34
C(4/II)	162.37	162.38	161.78[c])	161.9	162.02
C(5/II)	103.96	103.95	103.35	103.7	103.13
C(6/II)	151.34[b])	151.30	152.30[d])	152.27	152.01[b])
CH_2–C(6/II)	31.90[c])	31.51[e])	32.63	32.50[b])	32.21
C(1′/II)	92.80	91.24	90.76	91.56	91.94
C(2′/II)	85.06[d])	84.78[d])	84.12[e])	85.65[c])	71.27
C(3′/II)	84.46[d])	84.55[d])	83.36[e])	85.26[c])	72.27
C(4′/II)	91.32	89.89	89.10	91.03	82.43
C(5′/II)	31.54	32.93[e])	33.66	32.13[b])	33.83
Adenosine unit I					
C(2/I)	150.89	151.11	151.12	151.50	152.16
C(4/I)	150.96	150.35	149.52	149.71	150.12
C(5/I)	125.27	124.22	117.69	117.8	118.01
C(6/I)	151.12[b])	152.06[b])	155.68	155.03	155.61
C(8/I)	150.96	151.76[b])	150.65	149.92	151.06
CH_2–C(8/I)	59.86	59.74	56.78	58.12	56.57
C(1′/I)	89.54	89.89[c])	88.78	90.11	88.72
C(2′/I)	84.92[d])	83.88[d])	82.66[e])	84.61[c])	71.07[c])
C(3′/I)	84.31[d])	83.66[d])	83.45[e])	85.14[c])	72.43[d])
C(4′/I)	88.15	88.29	85.46	89.66	83.23[e])
C(5′/I)	32.68[c])	32.83[e])	33.66	31.94[b])	33.23

[a]) Assignment based on DQFCOSY, HSQC, and HMBC spectra. [b])–[e]) Assignment may be interchanged.

1037*s*, 1030*s*, 1011*m*. ^{1}H-NMR (300 MHz, (D_6)DMSO): see *Table 8*; additionally, 7.46–7.24 (*m*, 12 arom. H); 6.93 (*d*, *J* = 9.0, 2 arom. H); 6.68 (br. *s*, 2 NH_2); 3.75 (*s*, MeO); 1.52, 1.44, 1.41, 1.38, 1.30, 1.28, 1.25, 1.21 (8*s*, 4 Me_2C); 1.50–1.40 (hidden *sept.*, Me_2CH); 0.80 (*d*, *J* = 6.9, Me_2CH); 0.76 (*s*, Me_2CSi); 0.01, −0.01 (2*s*, Me_2Si); signals of H−N(3/II) and H−N(3/IV) hidden by the noise. HR-ESI-MS: 1735.652 (11), 1734.656 (14), 1733.648 (10, $[M+Na]^+$, $C_{82}H_{102}N_{14}NaO_{19}S_3Si^+$; calc. 1733.628), 1714.671 (12), 1713.671 (49), 1712.672 (89), 1711.679 (56, $[M+H]^+$, $C_{82}H_{103}N_{14}O_{19}S_3Si^+$; calc. 1711.646), 1462.465 (16), 1461.470 (25, $[M-MMTr+H+Na]^+$, $C_{62}H_{86}N_{14}NaO_{18}S_3Si^+$; calc. 1461.507), 1442.467 (12), 1441.468 (47), 1440.472 (80), 1439.479 (100, $[M-MMTr+2H]^+$, $C_{62}H_{87}N_{14}O_{18}S_3Si^+$; calc. 1439.525), 857.833 (80), 857.334 (22), 856.832 (45), 856.334 (45, $[M+2H]^{2+}$, $C_{82}H_{104}N_{14}O_{19}S_3Si^{2+}$; calc. 856.326).

5′-O-[Dimethyl(1,1,2-trimethylpropyl)silyl]-2′,3′-O-isopropylideneuridine-6-methyl-(6¹ → 5′-S)-2′,3′-O-isopropylidene-5′-thioadenosine-8-methyl-(8¹ → 5′-S)-2′,3′-O-isopropylidene-5′-thiouridine-6-methyl-(6¹ → 5′-S)-8-(hydroxymethyl)-2′,3′-O-isopropylidene-5′-thioadenosine (**25**). Under N_2, a soln. of **24** (30 mg, 17 μmol) in CH_2Cl_2 (1 ml) was treated with Cl_2CHCO_2H (100 μl, 1.22 mmol) and Et_3SiH (25 μl, 0.16 mmol), and stirred for 10 min at 23°. The mixture was poured into sat. $NaHCO_3$ soln. and extracted with CH_2Cl_2. The combined org. phases were washed with brine, dried ($MgSO_4$), and evaporated. Trituration of the crude material with MeOH gave **25** (15 mg, 60%). R_f (AcOEt/MeOH 92:8) 0.31. $[\alpha]^{25}_D = -29.1$ (*c* = 1.0, $CHCl_3$). UV ($CHCl_3$): 263 (45854). IR ($CHCl_3$): 3387*w* (br.), 3323*w*, 3171*w* (br.), 3015*w*, 2962*m*, 1710*s*, 1690*m*, 1647*m*, 1604*m*, 1443*w*, 1425*w*, 1377*m*, 1331*w*, 1298*w*, 1257*w*, 1157*w* (br.), 1089*m* (br.). ^{1}H-NMR (300 MHz, (D_6)DMSO): see *Table 8*; additionally, 11.40 (br. *s*, H−N(3/II), H−N(3/IV)); 7.31, 7.28 (2*s*, 2 NH_2); 5.80 (*t*, *J* = 5.7, *H*OCH_2−C(8/I); 1.52, 1.51, 1.43, 1.38, 1.29 (2 Me), 1.24, 1.21 (7*s*, 4 Me_2C); 1.50–1.40 (hidden *sept.*, Me_2CH); 0.79 (*d*, *J* = 6.9, Me_2CH); 0.76 (*s*, Me_2CSi); −0.01, −0.02 (2*s*, Me_2Si). ^{13}C-NMR (75 MHz, (D_6)DMSO): see *Table 9*; additionally, 113.19, 113.15, 112.38, 112.25 (4*s*, 4 Me_2C); 27.07, 26.97 (3 Me), 25.16 (3 Me), 24.75 (4*q*, 4 Me_2C); 25.06 (*s*, Me_2CSi); 20.23, 20.18 (2*q*, Me_2CH); 18.36, 18.32 (2*q*, Me_2CSi); −3.30, −3.37 (2*q*, Me_2Si). HR-ESI-MS: 731.763 (12), 731.262 (14, $[M+H+Na]^{2+}$, $C_{62}H_{87}N_{14}NaO_{18}S_3Si^{2+}$; calc. 731.258), 721.772 (15), 721.270 (49), 720.769 (83), 720.267 (100, $[M+2H]^{2+}$, $C_{62}H_{88}N_{14}O_{18}S_3Si^{2+}$, calc. 720.266). Anal. calc. for $C_{62}H_{86}N_{14}O_{18}S_3Si$ (1439.73): C 51.72, H 6.02, N 13.62; found: C 51.65, H 6.20, N 13.47.

2′,3′-O-Isopropylideneuridine-6-methyl-(6¹ → 5′-S)-2′,3′-O-isopropylidene-5′-thioadenosine-8-methyl-(8¹ → 5′-S)-2′,3′-O-isopropylidene-5′-thiouridine-6-methyl-(6¹ → 5′-S)-8-(hydroxymethyl)-2′,3′-O-isopropylidene-5′-thioadenosine (**26**). Under N_2, a soln. of **25** (35 mg, 24 μmol) in THF (1 ml) was treated with $(HF)_3 \cdot Et_3N$ (40 μl, 0.48 mmol), and stirred for 3 d at 23°. The mixture was poured into sat. $NaHCO_3$ soln., and extracted with CH_2Cl_2. The combined org. phases were washed with brine, dried ($MgSO_4$), and evaporated. The crude material was purified by trituration in acetone to yield **26** (11 mg, 35%). R_f (AcOEt/MeOH/H_2O 85:10:5) 0.26. $[\alpha]^{25}_D = -16.1$ (*c* = 1.0, $CHCl_3$). UV ($CHCl_3$): 263 (37451). IR ($CHCl_3$): 3386*w*, 3330*w*, 3195*w*, 3019*s*, 2928*m*, 28855*w*, 1702*s* (br.), 1657*m*, 1610*m*, 1444*w*, 1383*m*, 1378*m*, 1330*w*, 1301*w*, 1221*s*, 1213*s*, 1091*m*, 1073*m*. ^{1}H-NMR (600 MHz, 2°, $CDCl_3$; assignments based on DQF-COSY, TOCSY, and NOESY spectra): see *Table 8*; additionally, 14.20 (*s*, H−N(3/IV)); 13.07 (*s*, H−N(3/II)); 9.22, 7.47 (2*s*, H_2N−C(6/I)); 7.97, 5.66 (2*s*, H_2N−C(6/III)); 5.77 (br. *d*, *J* = 11.5, *H*OCH_2−C(8/I)); 4.69 (br. *d*, *J* = 9.7, HO−C(5′/IV)); 1.65, 1.40 (2*s*, Me_2C/I); 1.57, 1.39 (2*s*, Me_2C/II); 1.55, 1.29 (2*s*, Me_2C/III); 1.48, 1.29 (2*s*, 4 Me_2C/IV). ^{13}C-NMR (150 MHz, $CDCl_3$): see *Table 9*; additionally, 114.28, 113.80 (2*s*, 4 Me_2C); 27.47, 27.32, 27.23, 27.14, 25.76, 25.37, 25.26, 25.18 (8*q*, 4 Me_2C). HR-ESI-MS: 650.713 (11), 650.210 (35), 649.709 (64), 649.206 (100, $[M+2H]^{2+}$, $C_{54}H_{70}N_{14}O_{18}S_3^{2+}$; calc. 649.207).

Uridine-6-methyl-(6¹ → 5′-S)-5′-thioadenosine-8-methyl-(8¹ → 5′-S)-5′-thiouridine-6-methyl-(6¹ → 5′-S)-8-(hydroxymethyl)-5′-thioadenosine (**27**). A soln. of **26** (20 mg, 17 μmol) in CH_2Cl_2 (1 ml) was treated with CF_3CO_2H (1 ml) and H_2O (20 μl, 1.1 mmol), stirred for 1 h at 23°, and evaporated. The residue was triturated with acetone and neutralized (ion exchange resin *GC-120*) to afford **27** (9 mg, 52%). R_f (*RP-18*; MeOH/H_2O 1:1) 0.55. $[\alpha]^{25}_D = -20.7$ (*c* = 0.7, DMSO). IR (ATR): 3330*m* (br.), 3202*m* (br.), 1680*s* (br.), 1649*m*, 1608*m*, 1402*m*, 1384*m*, 1330*m*, 1308*m*, 1259*m*, 1094*m*, 1012*s*, 950*s*. ^{1}H-NMR (500 MHz, (D_6)DMSO; assignments based on DQF-COSY, HSQC, and HMBC spectra): see *Table 8*; additionally, 11.34, 11.31 (2*s*, H−N(3/II), H−N(3/IV)); 7.29 (br. *s*, 2 NH_2); 5.75 (br. *s*, $HOCH_2$−C(8/I)); 5.38 (br. *s*, HO−C(2′/I), HO−C(2′/III)); 5.33 (br. *s*, HO−C(3′/I), HO−C(3′/III)); 5.18 (br. *s*, HO−C(2′/II)); 5.13 (br. *s*, HO−C(2′/IV)); 5.07 (br. *s*, HO−C(3′/II)); 4.96 (br. *s*, HO−C(3′/IV)); 4.66 (br. *s*, HO−C(5′/IV)); ^{13}C-NMR (125 MHz, $CDCl_3$): see *Table 9*.

Determination of the Solution Structure of **26** *by NMR Spectroscopy.* a) *NMR Measurements.* 1D-^{1}H, 1D-^{13}C, as well as 2D DQF-COSY, TOCSY (DIPSI spin lock of 10 kHz, 80 ms) and NOESY (t_m 300 ms) spectra were recorded at 600 MHz (^{1}H) and 150 MHz (^{13}C). Because the duplex was kinetically too labile at r.t., all spectra were recorded at 2°. Residue-specific assignment of the H-atoms was achieved through a combination of COSY, TOCSY, and NOESY correlations.

b) *Derivation of Distance Constraints and Structure Calculation.* ^{1}H Assignments and volume integration of NOESY (mixing time 300 ms) cross-peaks were performed with the aid of SPARKY [20]. Distance constraints and error limits were generated from cross-peak volumes by calibration with known distances (two-spin approximation, ±20% error limits) through a python extension within SPARKY. The volume of cross-peaks involving Me groups or other isochronous H-atoms was corrected by division through the number of H-atoms. Distance restraints derived from NOESY were introduced into the simulated annealing calculations. Simulated annealing (SA) calculations were performed with XPLOR-NIH version 2.22 [15]. The parameter-file parnah1er1_mod_new.inp and the topology-file topalldna.hdg [21] were modified to accomodate the new CH_2SCH_2 linkers (equilibrium values for bonds and angles were based on the X-ray structure of a closely related dimer [3]). All other parameters concerning base and sugar atoms as well as force constants (k_{bond} = 1000 kcal/mol, k_{angle} = 500 kcal/mol, $k_{improper}$ = 500 kcal/mol) were left unchanged. The only nonbonded interaction used was a *Van der Waals* repel function.

Two antiparallelly oriented random conformation single strands were used as the starting structure. The SA protocol (adopted from torsion-angle dynamics protocol of *Stein et al.* [22]) included 4000 steps (0.015 ps each) of high temp. torsion-angle dynamics at 20000 K, followed by 4000 (0.015 ps) steps of slow cooling to 1000 K with torsion-angle dynamics, 2000 steps (0.003 ps) of slow cooling with *Verlet* dynamics to 300 K, followed by a final *Powell* minimization.

The chemical shift of H–N(3) and their inter-strand NOEs to H–C(2) indicate that they are involved in either *Watson–Crick* or reverse *Watson–Crick* base pairing. Therefore, H-bonding within base pairs was initially defined by only a single central H-bond restraint rather than a double H-bond restraint so as to allow the NOE constraints to generate base-pairs in either *Watson–Crick* or reverse *Watson–Crick* manner. After obtaining a structure with no NOE violations which showed uniform *Watson–Crick* pairing, a second H-bond as well as planarity restraints keeping the base pairs planar were introduced before calculating the final ensemble of structures. 97 Structures were generated using the SA protocol as explained above. 64 Structures, which showed no NOE violation > 0.1 Å, no deviation from equilibrium value for bond lengths, bond angles, and improper angles of > 0.05 Å, > 5.0°, and > 1.5°, respectively, were accepted.

To verify that the generated antiparallel, fully *Watson–Crick*-paired duplex was not the result of limited sampling of conformational space, three parallel calculations were performed using the same NOE constraints but replacing the H-bond restraints file to enforce the three other possible C_2-symmetric combinations of *Watson–Crick* (*WC*) or reverse *Watson–Crick* (r*WC*) pairing modes. I: All H-bonds between base pairs were set to r*WC*. II: The H-bonds between terminal base pairs were set to r*WC* and the two central base pairs to *WC*. III: The H-bonds between central base pairs were set to r*WC* and the two terminal base pairs to *WC*. In all three control calculations, none of the generated structures was within the acceptance limits for NOE-constraint violations, thus confirming the *Watson–Crick* pairing mode for all four base pairs of **26**.

REFERENCES

[1] N. Bogliotti, A. Vasella, *Helv. Chim. Acta* **2009**, *92*, 1167.
[2] X. Zhang, B. Bernet, A. Vasella, *Helv. Chim. Acta* **2006**, *89*, 2861.
[3] A. Ritter, D. Egli, B. Bernet, A. Vasella, *Helv. Chim. Acta* **2008**, *91*, 673.
[4] X. Zhang, B. Bernet, A. Vasella, *Helv. Chim. Acta* **2007**, *90*, 792.
[5] H. Tanaka, H. Hayakawa, T. Miyasaka, *Tetrahedron* **1982**, *38*, 2635; K. Hirota, Y. Kitade, F. Iwami, S. Senda, *Chem. Pharm. Bull.* **1984**, *32*, 2591; M. P. Groziak, R. Lin, *Tetrahedron* **2000**, *56*, 9885.
[6] J. Hollmann, E. Schlimme, *Liebigs Ann. Chem.* **1984**, 98; T. Ueda, Y. Nomoto, A. Matsuda, *Chem. Pharm. Bull.* **1985**, *33*, 3263.

[7] H. S. Gutowsky, A. Saika, *J. Chem. Phys.* **1953**, *21*, 1688.
[8] A. Ritter, B. Bernet, A. Vasella, *Helv. Chim. Acta* **2008**, *91*, 1675.
[9] P. K. Bhardwaj, A. Vasella, *Helv. Chim. Acta* **2002**, *85*, 699.
[10] F. Mohamadi, N. G. J. Richards, W. C. Guida, R. Liskamp, C. Caufield, M. Lipton, G. Chang, T. Hendrickson, W. C. Still, *J. Comput. Chem.* **1990**, *11*, 440.
[11] 'Spartan 04 on Macintosh', *Wavefunction, Inc.*, Irvine, CA, USA.
[12] F. Cordier, M. Barfield, S. Grzesiek, *J. Am. Chem. Soc.* **2003**, *125*, 15750.
[13] R. Vargas, J. Garza, D. A. Dixon, B. P. Hay, *J. Am. Chem. Soc.* **2000**, *122*, 4750.
[14] X. Zhang, B. Bernet, A. Vasella, *Helv. Chim. Acta* **2007**, *90*, 864.
[15] C. D. Schwieters, J. J. Kuszewski, N. Tjandra, G. M. Clore, *J. Magn. Reson.* **2003**, *160*, 65.
[16] Z. Johar, Thesis ETH Zürich No. 17256, 2007, pp. 39 – 51.
[17] A. J. Matthews, P. K. Bhardwaj, A. Vasella, *Helv. Chim. Acta* **2004**, *87*, 2273.
[18] S. Eppacher, N. Solladié, B. Bernet, A. Vasella, *Helv. Chim. Acta* **2000**, *83*, 1311.
[19] W. J. Cook, S. E. Ealick, J. A. Secrist III, *Acta Crystallogr., Sect. C: Cryst. Struct. Commun.* **1984**, *40*, 885.
[20] T. D. Goddard, D. G. Kneller, 'Program SPARKY v3.110', University of California, San Francisco, 2004.
[21] http://spin.niddk.nih.gov/clore.
[22] E. G. Stein, L. M. Rice, A. T. Brünger, *J. Magn. Reson.* **1997**, *124*, 154.

Received May 29, 2009